Lowry, O.H., Rosebrough, N.J., Farr, A.L., Randall, R.J., 1951. Protein measurement with the Folin phenol reagent. J. Biol. Chem. 193, 265–275.
Luquita, M.G., Catania, V.A., Pozzi, E.J.S., Veggi, L.M., Hoffman, T., Pellegrino, J.M., Ikushiro, S., Emi, Y., Iyanagi, T., Vore, M., Mottino, A.D., 2001. Molecular basis of perinatal changes in UDP-glucuronosyltransferase activity in maternal rat liver. J. Pharmacol. Exp. Ther. 298, 49–56.
Masuda, Y., 2009. Toxic effects of PCB/PCDF to human observed in Yusho and other poisonings. Fukuoka Acta Med. 100, 141–155.
McFarland, V.A., Clarke, J.U., 1989. Environmental occurrence, abundance, and potential toxicity of polychlorinated biphenyl congeners: considerations for a congener-specific analysis. Environ. Health Perspect. 81, 225–239.
Meerts, I.A.T.M., Assink, Y., Cenijn, P.H., van den Berg, J.H.J., Weijers, B.M., Bergman, Å., Koeman, J.H., Brouwer, A., 2002. Placental transfer of a hydroxylated polychlorinated biphenyl and effects on fetal and maternal thyroid hormone homeostasis in the rat. Toxicol. Sci. 68, 361–371.
Ness, D.K., Schantz, S.L., Moshtaghian, J., Hansen, L.G., 1993. Effects of perinatal exposure to specific PCB congeners on thyroid hormone concentrations and thyroid histology in the rat. Toxicol. Lett. 68, 311–323.
Oppenheimer, J.H., Bernstein, G., Surks, M.I., 1968. Increased thyroxine turnover and thyroidal function after stimulation of hepatocellular binding of thyroxine by phenobarbital. J. Clin. Invest. 47, 1399–1406.
Pizzagalli, F., Hagenbuch, B., Stieger, B., Klenk, U., Folkers, G., Meier, P.J., 2002. Identification of a novel human organic anion transporting polypeptide as a high affinity thyroxine transporter. Mol. Endocrinol. 16, 2283–2296.
Safe, S.H., 1990. Polychlorinated biphenyls (PCBs), dibenzo-*p*-dioxins (PCDDs), dibenzofurans (PCDFs), and related compounds: environmental and mechanistic considerations which support the development of toxic equivalency factors (TEFs). Crit. Rev. Toxicol. 21, 51–88.
Schuur, A.G., Boekhorst, F.M., Brouwer, A., Visser, T.J., 1997. Extrathyroidal effects of 2,3,7,8-tetrachlorodibenzo-*p*-dioxin on thyroid hormone turnover in male Sprague–Dawley rats. Endocrinology 138, 3727–3734.
Ucán-Marín, F., Arukwe, A., Mortensen, A., Gabrielsen, G.W., Fox, G.A., Letcher, R.J., 2009. Recombinant transthyretin purification and competitive binding with organohalogen compounds in two gull species (*Larus argentatus* and *Larus hyperboreus*). Toxicol. Sci. 107, 440–450.
Van Birgelen, A.P.J.M., Smit, E.A., Kampen, I.M., Groeneveld, C.N., Fase, K.M., van der Kolk, J., Poiger, H., van den Berg, M., Koeman, J.H., Brouwer, A., 1995. Subchronic effects of 2,3,7,8-TCDD or PCBs on thyroid hormone metabolism: use in risk assessment. Eur. J. Pharmacol. 293, 77–85.
Vansell, N.R., Klaassen, C.D., 2001. Increased biliary excretion of thyroxine by microsomal enzyme inducers. Toxicol. Appl. Pharmacol. 176, 187–194.
Visser, T.J., 1996. Pathways of thyroid hormone metabolism. Acta Med. Austriaca 23, 10–16.

Food and Chemical Toxicology 49 (2011) 2167–2171

Contents lists available at ScienceDirect

Food and Chemical Toxicology

journal homepage: www.elsevier.com/locate/foodchemtox

Transcellular transport of domoic acid across intestinal Caco-2 cell monolayers

Osamu Kimura [a], Yuichi Kotaki [b], Naoya Hamaue [a], Koichi Haraguchi [c], Tetsuya Endo [a,*]

[a] Faculty of Pharmaceutical Sciences, Health Sciences University of Hokkaido, 1757 Ishikari-Tobetsu, Hokkaido 061-0293, Japan
[b] School of Marine Biosciences, Kitasato University, Sanriku, Ofunato 022-0101, Japan
[c] Daiichi College of Pharmaceutical Sciences, 22-1 Tamagawa-Cho, Minami-Ku, Fukuoka 815-8511, Japan

ARTICLE INFO

Article history:
Received 18 October 2010
Accepted 1 June 2011
Available online 6 June 2011

Keywords:
Domoic acid
Intestinal transport
Caco-2 cells
Chloride ions
DIDS (4,4′-diisothiocyanostilbene-2,2′-disulfonic acid)

ABSTRACT

The intestinal absorption mechanism of domoic acid (DA) was investigated using Caco-2 cells. DA is a tricarboxylic amino acid that contains a glutamic acid moiety, and causes deficits in short-term memory by binding to glutamate receptors as an agonist of glutamic acid. Caco-2 cell monolayers cultured on permeable membranes were incubated with 100 μM DA on either the apical or basolateral side, and the transcellular transport of DA was measured. The transcellular transport of DA from the apical to basolateral side was about twofold that in the opposite direction. The transcellular transport of DA from the apical side was optimal at a neutral pH, and was temperature- and Cl^--dependent, but was Na^+-independent. Coincubation of DA with 4,4′-diisothiocyanostilbene-2,2′-disulfonic acid (DIDS), an anion exchange inhibitor, significantly decreased the apical-to-basolateral transport of DA by 48%, and coincubation with probenecid (a non-specific anion transport inhibitor) significantly decreased the transport of DA by 31%. In contrast, coincubation with glutamic acid, succinic acid (a dicarboxylic acid), or citric acid (a tricarboxylic acid) did not decrease the transport of DA. These results suggest that the apical-to-basolateral transport of DA across the Caco-2 cell monolayers is mediated by DIDS-sensitive anion transporters.

1. Introduction

Domoic acid (DA) is a potent excitotoxin produced by various marine algae and diatoms, and it has been found in marine wildlife throughout the world via the food web (Lefebvre and Robertson, 2010). DA is a tricarboxylic amino acid that contains glutamic acid moiety, and causes deficits in short-term memory by binding to glutamate receptors in the hippocampus as an agonist of glutamic acid (Wright et al., 1989; Hampson et al., 1992; Lefebvre and Robertson, 2010).

As most studies on DA using experimental animals have focused on the mechanisms of neurotoxicity, limited information is available on the intestinal absorption, distribution, metabolism, and excretion (ADME) of DA after ingestion. Truelove and Iverson (1994) investigated the pharmacokinetics of DA in monkeys and rats after intravenous dosing, and reported the rapid excretion of DA: the plasma half-life for DA was 114.5 min in monkeys and 21.6 min in rats. Suzuki and Hierlihy (1993) investigated the excretion of DA in rats after intravenous dosing, and reported that DA was completely recovered in the urine within 160 min and that this excretion was not affected by treatment with probenecid, a competitive inhibitor of renal anion transport systems. The absorption rate of DA, estimated from the urinary excretion of DA after oral administration, was trace in both monkeys (4–7%) and rats (1.8%) (Truelove et al., 1996, 1997).

Ross et al. (2000) investigated the effects of DA on the uptake of glutamic acid in rat astrocytes, and reported that DA inhibited the uptake of glutamic acid in a dose-dependent manner. Some research groups reported that the uptake of glutamic acid across intestinal brush border membranes is predominantly mediated by a Na^+-dependent transport system (Rajendran et al., 1987; Nicklin et al., 1995; Mordrelle et al., 2000). These results led us to the hypothesis that DA absorption is mediated via the same transporter as that for glutamic acid. Furthermore, the possibility of DA absorption via monocarboxylic, dicarboxylic, or tricarboxylic acid transporter(s) as well as other transporters can be speculated.

In the present study, we investigated the absorption mechanism of DA using Caco-2 cells, which are morphologically and functionally similar to human small intestinal epithelial cells and widely used to predict intestinal "*in vivo*" absorption in humans (Hilgers et al., 1990).

2. Materials and methods

2.1. Materials

Dulbecco's modified Eagle's medium (DMEM), glycylsarcosine, benzoic acid, glutaric acid, acetic acid, succinic acid, citric acid, *p*-aminohippuric acid, tetraethylammonium, probenecid, L-proline, L-leucin, L-lysine, L-tryptophan were purchased from Wako Pure Chemical Industries, Ltd. (Osaka, Japan). L-Lactic acid, L-alanine, L-glutamic acid, L-asparatic acid, sulfobromophthalein, estron-3-sulfate, γ-aminobu-

* Corresponding author. Tel./fax: +81 0133 23 3902.
E-mail address: endotty@hoku-iryo-u.ac.jp (T. Endo).

0278-6915/$ - see front matter © 2011 Elsevier Ltd. All rights reserved.
doi:10.1016/j.fct.2011.06.001

tyric acid, 4,4′-diisothiocyanostilbene-2,2′-disulfonic acid (DIDS) were purchased from Sigma Chemical Co. (St. Louis, MO). Fetal bovine serum (FBS) and nonessential amino acid (NEAA) were obtained from Life Technologies (Rockville, MD). All other chemicals were commercial products of reagent grade.

Domoic acid (DA) was extracted with hot water from the red alga *Chondria armata* collected in July 2007 in Kagoshima Prefecture, Japan. The extract was purified by successive column chromatographies (3 × 45 and 2 × 45 cm) packed with reversed-phase silica gel (Wakosil 25 C18, Wako Pure Chemical Industries, Ltd., Osaka, Japan) and preparative HPLC with a Develosil ODS-5 column (1 × 25 cm, Nomura Chemical Co. Ltd., Seto, Japan). The mobile phase of 1% acetic acid in 10% acetonitrile was mainly used for purification. DA was monitored during the purification process by HPLC with UV detection (242 nm) according to a slightly modified version of Quilliam's method (Quilliam et al., 1989; Kotaki et al., 1999) in which a Develosil ODS-5 column (4.6 × 250 mm) with a mobile phase of 10% acetonitrile in 20 mM NaH_2PO_4 buffer (pH 2.5) was used. DA of 95% purity was obtained by above purification procedures. Absence of isomers such as isodomoic acids A and B and 5′-epi-domoic acid was also confirmed by HPLC analysis.

2.2. Cell culture

Caco-2 cells were obtained from RIKEN Cell Bank (Tsukuba, Japan) at passage 40, and used between passages 50 and 85. Caco-2 cells were cultured on permeable membranes (Cell Culture Insert, 0.4 μm, 0.9 cm^2 growth area; Becton Dickinson, Bedford, MA) in DMEM containing FBS (10%), NEAA (1%), streptomycin (100 μg/mL) and penicillin G (70 μg/mL) at 37 °C under a humidified atmosphere of 5% CO_2–95% air. The volume of culture medium on the apical and basolateral sides was 0.5 and 1.5 mL, respectively, and the medium was replaced every 2 or 3 days after seeding.

2.3. Transport experiments

Confluent cultures of Caco-2 cell monolayers (cultured for 21 or 22 days) with the transepithelial electrical resistances (TERs) of more than 350 Ω cm^2 were used for the transport experiments. These experiments were performed as described previously (Kimura et al., 2005, 2009). Briefly, the culture medium was replaced with the same volume of incubation medium, and the cell monolayers were preincubated at 37 °C or 4 °C for 20 min. The incubation medium used for the transport study was Hanks' balanced salt solution (137 mM NaCl, 5.36 mM KCl, 0.952 mM $CaCl_2$, 0.812 mM $MgSO_4$, 0.441 mM KH_2PO_4, 0.385 mM Na_2HPO_4) containing 25 mM D-glucose and 10 mM MES (pH 5.5, 6.0 or 6.5) or 10 mM HEPES (pH 7.0, 7.4 or 8.0). After preincubation, the cell monolayers were incubated with 100 μM DA in fresh incubation medium from either the apical or basolateral side for the indicated times at 37 °C or 4 °C.

In order to investigate the Na^+ dependence of the transcellular transport of DA, NaCl in the incubation medium was replaced with equimolar choline chloride or KCl, and Na_2HPO_4 was omitted from the medium. Furthermore, the cell monolayers were pretreated with 0.5 mM ouabain, a Na/K-ATPase inhibitor (Nicklin et al., 1995; Kimura et al., 1996), before incubation with DA. To examine the effect of an anion exchange inhibitor, the cell monolayers were coincubated at 37 °C for 60 min with 100 μM DA and 0.1 or 1.0 mM DIDS (Ogihara et al., 1999). To examine the effect of Cl^-, NaCl, KCl and $CaCl_2$ in the incubation medium were replaced with their respective gluconate salts. In the inhibition study, the cell monolayers were coincubated at 37 °C for 60 min with 100 μM DA and various compounds from the apical side.

2.4. Determination of domoic acid

DA was determined using an HPLC system consisting of a Shimadzu LC-10A pump and SPD-10A UV detector. The analytical conditions were as follows: column, Inertsil VP-ODS (4 × 250 mm; GL Sciences, Inc., Tokyo, Japan); mobile phase, 20 mM NaH_2PO_4 buffer (pH 2.5)/acetonitorile (90:10 (v/v)); flow rate, 0.8 mL/min; wavelength, 242 nm.

2.5. Statistical analyses

The data were analyzed by either Student's *t*-test or Scheffe's multiple comparison test after analysis of variance using the Statcell 12 program. The level of significance was set at $p < 0.05$.

3. Results

3.1. Time course of domoic acid transport across Caco-2 cell monolayers

The time course of the transcellular transport of DA across Caco-2 cell monolayers was investigated. Caco-2 cells were incubated at 37 °C with 100 μM DA from either the apical or basolateral side (Fig. 1). The transcellular transport of DA from the apical to basolateral side and from the basolateral to apical side increased linearly until 60 min. The apical-to-basolateral transport of DA was about twofold that in the opposite direction. As a result of the preferential transport of DA, further studies were focused on the apical-to-basolateral transport.

3.2. Effect of apical pH on the transcellular transport of domoic acid across Caco-2 cell monolayers

Caco-2 cell monolayers were incubated in incubation medium containing 100 μM DA on the apical side at 37 °C for 60 min at different pH values (Fig. 2). A change in pH from 7.4 to 6.4 did not affect the transcellular transport of DA, but DA transport at pH 5.5 (88.8%) and pH 8.0 (74.1%) was significantly lower than that at pH 7.4.

3.3. Effects of temperature and sodium on the transcellular transport of domoic acid across Caco-2 cell monolayers

The effects of low temperature and Na^+ on the transcellular transport of DA were examined (Fig. 3). Incubation at low temperature (4 °C) significantly reduced the transcellular transport of DA by 75.0%; however, Na^+-free conditions, achieved by the replacement of NaCl in incubation medium with equimolar choline chloride or KCl, did not decrease the transcellular transport of DA. In addition, pretreatment with 0.5 mM ouabain, a Na^+/K^+-ATPase inhibitor, did not decrease the transport of DA.

3.4. Effects of DIDS and chloride ions on the transcellular transport of domoic acid across Caco-2 cell monolayers

Transcellular transport of DA from the apical membrane via the anion exchanger was investigated (Fig. 4). Coincubation with DIDS, an anion exchange inhibitor, significantly inhibited the transcellular transport of DA in a dose-dependent manner: coincubation with 0.1 and 1.0 mM DIDS caused a 19.6 and 47.8% inhibition of DA transport, respectively.

The effect of Cl^- on the transcellular transport of DA was also examined (Fig. 5). The replacement of Cl^- by gluconate ions in the incubation medium on the apical side slightly but significantly decreased DA transport, and coincubation with DIDS caused a further decrease in DA transport. The replacement of Cl^- in the medium on both the apical and basolateral sides markedly decreased

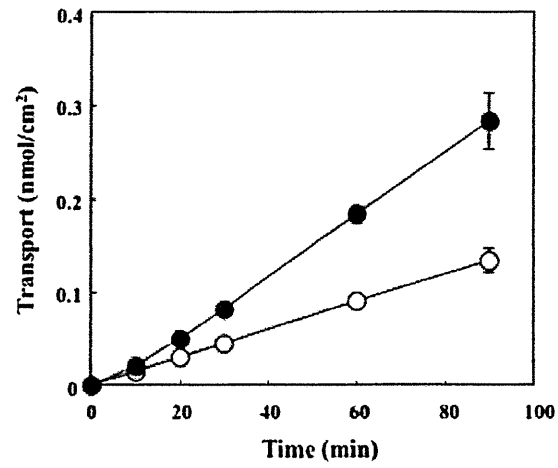

Fig. 1. Time course of domoic acid transport across Caco-2 cell monolayers. Caco-2 cell monolayers were incubated at 37 °C with 100 μM domoic acid added to the apical or basolateral medium. Each point represents the mean with S.E. for 3–6 determinations.

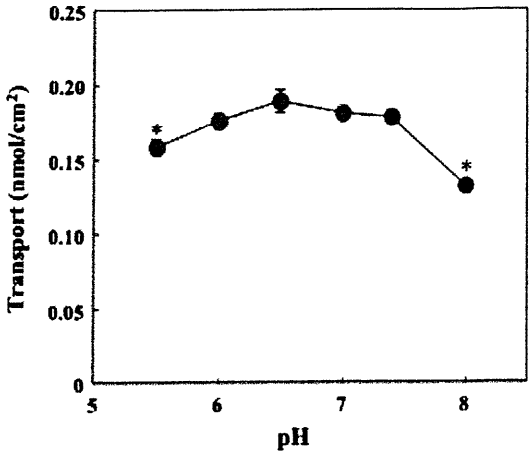

Fig. 2. Transcellular transport of domoic acid across Caco-2 cell monolayers at various pH values of the apical medium. Caco-2 cell monolayers were incubated at 37 °C for 60 min with 100 μM domoic acid added to the apical medium at various pH values. The pH of the basolateral medium was maintained at pH 7.4. Each point represents the mean with S.E. for five or six monolayers. *Significantly different from the apical medium at pH 7.4.

DA transport by 45.6%, and this decrease in DA transport was the same as that caused by coincubation with 1.0 mM DIDS (Fig. 4).

3.5. Effects of various compounds on the transcellular transport of domoic acid across Caco-2 cell monolayers

In order to characterize the transport system responsible for the apical-to-basolateral transport of DA, the effects of various compounds on DA transport were examined (Table 1). Coincubation with probenecid, a non-specific inhibitor of anion transport, significantly decreased the apical-to-basolateral transport of DA by 31.5%. In contrast, coincubation with tetraetylammonium, a typical substrate of organic cation transport systems (OCTs), and *p*-aminohippuric acid, a typical substrate of organic anion transport systems (OATs), did not decrease the transport of DA. Amino acids (L-leucin, L-proline, L-tryptophan, L-asparatic, L-glutamic and γ-aminobutyric acids), monocarboxylic acids (L-lactic, acetic and

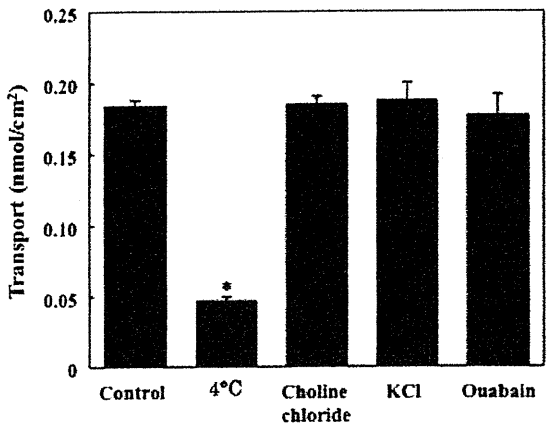

Fig. 3. Effects of temperature and sodium of transcellular transport of domoic acid across Caco-2 cell monolayers. Caco-2 cell monolayers were preincubated with 0.5 mM ouabain from both the apical and basolateral sides at 37 °C for 30 min. The cell monolayers were incubated with 100 μM domoic acid in HBSS, or sodium-trace HBSS (choline chloride and KCl) from the apical side at 4 or 37 °C for 60 min. Each point represents the mean with S.E. for five or six monolayers. *Significantly different from control.

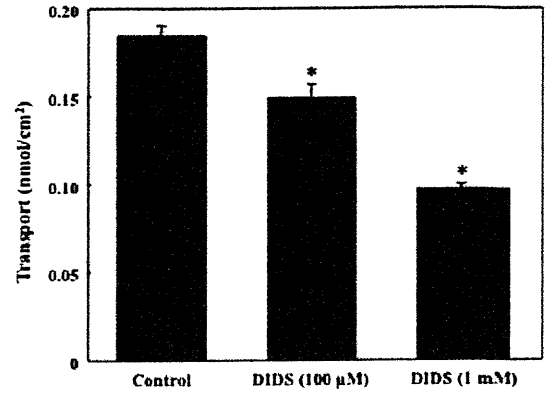

Fig. 4. Effect of DIDS on the transcellular transport of domoic acid across Caco-2 cell monolayers. Caco-2 cell monolayers were incubated at 37 °C for 60 min with 100 μM domoic acid added to the apical medium at pH 7.4 in the presence or absence of 0.1 or 1.0 mM DIDS. Each point represents the mean with S.E. for six monolayers. *Significantly different from the control.

benzoic acids), dicarboxylic acids (glutaric and succinic acids), tricarboxylic acid (citric acid), estrone-3-sulfate and sulfobromophthalein (substrates of the organic anion transporting polypeptide family; OATPs) and glycylsarcosine (a substrate of peptide transporters) did not decrease the apical-to-basolateral transport of DA (Table 1).

4. Discussion

We investigated the transcellular transport mechanism of DA using Caco-2 cell monolayers cultured on permeable membranes. The transcellular transport of DA from the apical to basolateral side was about twofold that in the opposite direction (Fig. 1). The transcellular transport of DA from the apical side was both temperature- and Cl^--dependent, and optimal at neutral pH, but was Na^+-independent (Figs. 2 and 3). In addition, the transport of DA from the apical to basolateral side was significantly decreased (approx. 50%) by coincubation with 1.0 mM DIDS (Fig. 4): the preferential direction of DA transport was diminished by the coincubation with

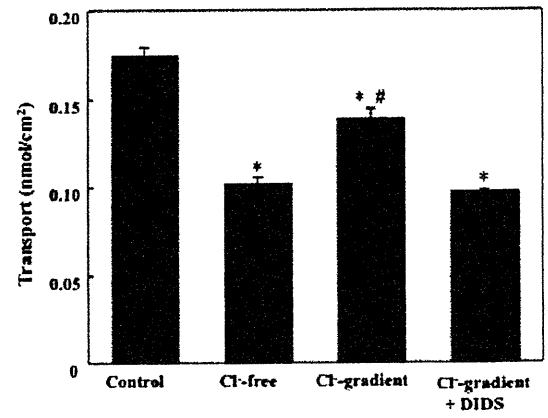

Fig. 5. Effect of chloride ion gradient on the transcellular transport of domoic acid across Caco-2 cell monolayers. Caco-2 cell monolayers were incubated at 37 °C for 60 min with 100 μM domoic acid added to the apical medium at pH 7.4 in the presence or absence of 1.0 mM DIDS. Cl^--free conditions: chloride ion-free apical and basolateral media, Cl^--gradient conditions: chloride ions-free apical medium. Each point represents the mean with S.E. for six monolayers. *Significantly different from the control. #Significantly different from the Cl^--free conditions or from the Cl^--gradient with DIDS.

Table 1
Effects of various compounds on the transcellular transport of domoic acid across Caco-2 cell monolayers.

Compound	Concentration (mM)	Domoic acid transport (% of control)
Control		100.0 ± 4.59
Tetraethylammonium	10	99.5 ± 3.54
p-Aminohippuric acid	10	97.8 ± 2.79
Probenecid	10	68.5 ± 2.76*
Succinic acid	10	97.3 ± 4.16
Glutaric acid	10	83.4 ± 2.82
Citric acid	10	87.6 ± 2.11
L-Lactic acid	10	88.1 ± 2.43
Acetic acid	10	89.9 ± 3.87
Benzoic acid	10	87.5 ± 5.07
Sulfobromophtalein	1	88.0 ± 4.25
Estrone-3-sulfate	1	90.3 ± 2.39
L-Asparatic acid	10	85.8 ± 3.75
L-Glutamic acid	10	85.7 ± 2.52
L-Alanine	10	84.6 ± 1.93
L-Proline	10	88.7 ± 4.87
L-Leucin	10	83.1 ± 3.92
L-Lysine	10	97.2 ± 2.76
L-Tryptophan	10	89.5 ± 4.56
γ-Aminobutyric acid	10	91.4 ± 3.86
Glycylsarcosine	10	93.6 ± 4.03

Caco-2 cell monolayers were coincubated with 100 μM domoic acid and various compounds on the apical side at 37 °C for 60 min. Each point represents the mean ± S.E. of 5–7 monolayers.
* Significantly different from the control.

DIDS. These results suggest that the transcellular transport of DA from the apical side is mediated by DIDS-sensitive anion transport systems. Anion exchangers (AEs) mediate the exchange of anions such as Cl^- and HCO_3^-. AEs are expressed in the intestine and Caco-2 cells (Alrefai et al., 2001; Jacob et al., 2002; Lecona et al., 2008), and inhibited by DIDS (Ogihara et al., 1999; Jacob et al., 2002). In the present study, the transport of DA was decreased by the replacement of Cl^- in the incubation media and the coincubation with DIDS (Fig. 5). These results imply that the transcellular transport of DA from the apical membrane is mediated by a DA/Cl^- antiporter, though further study using brush border membrane vesicles isolated from the small intestine is necessary to elucidate whether the intestinal absorption of DA is mediated by a DA/Cl^- antiporter.

DA is an amino acid with three carboxylic groups and one imino group in its structure, and structurally resembles glutamic acid, acting as a potent glutamate receptor agonist (Hampson et al., 1992; Lefebvre and Robertson, 2010). Glutamic acid uptake across intestinal brush border membranes purified from the human intestine and Caco-2 cells is mediated predominantly by a Na^+-dependent transport system (Rajendran et al., 1987; Nicklin et al., 1995; Mordrelle et al., 2000). However, the transcellular transport of DA across the apical membrane of Caco-2 cells was Na^+-independent (Fig. 3), and coincubation with 10 mM glutamic acid did not decrease DA transport, suggesting that DA does not share the same transporter as glutamic acid. On the other hand, Mordrelle et al. (1997) reported that the transport of glutamic acid in the rat intestinal crypt-like cell line IEC-17 was mediated not only by Na^+-dependent, but also by Na^+-independent transport systems, and coincubation with L-cystine, a substrate for Na^+-independent transport systems, significantly decreased the uptake of glutamate under Na^+-free conditions. In the present study, coincubation with L-cystine did not decrease the apical-to-basolateral transport of DA under Na^+-free conditions (data not shown), suggesting that the Na^+-independent transport system is not responsible for the intestinal absorption of DA. Although other amino acid transporters and dipeptide transporters are expressed in Caco-2 cells, similar to the intestine (Tsuji and Tamai, 1996; Hilgendorf et al., 2007), no significant inhibition of DA transport was observed by coincubation with neutral, basic or aromatic amino acids, or glycylsarcosine (a typical substrate of peptide transporters) (Table 1). These results suggest that the transcellular transport of DA across Caco-2 cells is not mediated by amino acid or peptide transporters.

OATPs are reported to be expressed in and localized at the brush border membrane of both the human small intestine and Caco-2 cells, where they mediate the transport of estrone-3-sulfate and sulfobromophtalein under acidic conditions (Sai et al., 2006). In the present study, coincubation with estrone-3-sulfate or sulfobromophtalein did not decrease DA transport (Table 1), and the transport of DA from apical side was lower under acidic conditions (Fig. 2). OATPs appear not to be involved in the transcellular transport of DA from the apical side in Caco-2 cells.

Uptake of citrate (a tricarboxylate) from the apical membrane of Caco-2 cells is reported to be mediated by transporters, and uptake of dicarboxylic compounds, such as succinic and glutaric acid, is also reported to be mediated by dicarboxylic transporters (Weerachayaphorn and Pajor, 2008). However, coincubation with citric acid, succinic acid or glutaric acid did not affect DA transport (Table 1). Thus, DA transport may not share the same transporter as tricarboxylic or dicarboxylic acids.

It has been reported that various monocarboxylic acid transport family (MCTs) isoforms (MCT1 and MCT3–MCT6) are expressed in Caco-2 cells, of which H^+-linked MCT1 is the most abundant (Hadjiagapiou et al., 2000). However, the optimal pH of the transport of DA from the apical side occurred under neutral conditions (Fig. 2), and was not inhibited by the presence of monocarboxylic acids (Table 1), suggesting that MCTs are not responsible for the transcellular transport of DA.

We previously reported that the uptake of 4-chloro-2-methylphenoxyacetic acid (MCPA) in Caco-2 cells is mediated via MCTs (Kimura et al., 2008, 2009), of which the absorption rate was reported to be notably high (Lappin et al., 2002). The apical-to-basolateral transport of MCPA (50 μM) at 60 min and pH 6.0 under the same conditions of the present experiment was about 5.9 nmol/cm^2 (our unpublished data). In contrast, the transport of DA (100 μM) at 60 min and pH 7.4 was markedly lower (about 0.18 nmol/cm^2, Fig. 1), and the absorption rate of DA was reported to be trace (Truelove et al., 1996, 1997). Thus the contribution of DIDS-sensitive transport in "*in vivo* absorption of DA" may be small.

Coincubation with tetraethylammonium (a typical substrate of OCTs) or *p*-aminohippuric acid (a typical substrate of OATs) did not decrease the transport of DA, although DA is a zwitterion at a physiological pH.

In conclusion, we elucidated the contribution of DIDS-sensitive transport in DA transport in Caco-2 cells, although the absorption rates of DA in experimental animals were reported to be trace (Truelove et al., 1996, 1997). Against expectations, DA transport appears not to share a transport system with glutamic acid.

Conflict of Interest

The authors declare that there are no conflicts of interest.

Acknowledgments

This work was supported by Grants-in-Aid from Japan Society for the Promotion of Science (C21590135) and International Fund for Animal Welfare (IFAW).

References

Alrefai, W.A., Tyagi, S., Nazir, T.M., Barakat, J., Anwar, S.S., Hadjiagapiou, C., Bavishi, D., Sahi, J., Malik, P., Goldstein, J., Layden, T.J., Ramaswamy, K., Dudeja, P.K., 2001. Human intestinal anion exchanger isoforms: expressio, distribution, and membrane localization. Biochim. Biophys. Acta 1511, 17–27.

Hadjiagapiou, C., Schmidt, L., Dudeja, P.K., Layden, T.J., Ramaswamy, K., 2000. Mechanism(s) of butyrate transport in Caco-2 cells: role of monocarboxylate transporter 1. Am. J. Physiol. Gastrointest. Liver Physiol. 279, G775–G780.

Hampson, D.R., Huang, X.P., Wells, J.W., Walter, J.A., Wright, J.L., 1992. Interaction of domoic acid and several derivatives with kainic acid and AMPA binding sites in rat brain. Eur. J. Pharmacol. 218, 1–8.

Hilgendorf, C., Ahlin, G., Seithel, A., Artursson, P., Ungell, A.L., Karlsson, J., 2007. Expression of thirty-six drug transporter genes in human intestine, liver, kidney, and organotypic cell lines. Drug Metab. Dispos. 35, 1333–1340.

Hilgers, A.R., Conradi, R.A., Burton, P.S., 1990. Caco-2 cell monolayers as a model for drug transport across the intestinal mucosa. Pharm. Res. 7, 902–910.

Jacob, P., Rossmann, H., Lamprecht, G., Kretz, A., Neff, C., Lin-Wu, E., Gregor, M., Groneberg, D.A., Kere, J., Seidler, U., 2002. Down-regulated in adenoma mediates apical Cl^-/HCO^{3-} exchange in rabbit, rat, and human duodenum. Gastroenterology 122, 709–724.

Kimura, O., Endo, T., Sakata, M., 1996. Comparison of cadmiun uptakes from apical and basolateral membranes of LLC-PK_1 cells. Toxicol. Appl. Pharmacol. 137, 301–306.

Kimura, O., Endo, T., Hotta, Y., Sakata, M., 2005. Effects of P-glycoprotein inhibitors on transepithelial transport of cadmium in cultured renal epithelial cells, LLC-PK_1 and LLC-GA5-COL 150. Toxicology 208, 123–132.

Kimura, O., Tsukagoshi, K., Endo, T., 2008. Uptake of 4-chloro-2-methylphenoxyacetic acid (MCPA) from the apical membrane of Caco-2 cells by the monocarboxylic acid transporter. Toxicol. Appl. Pharmacol. 227, 325–330.

Kimura, O., Tsukagoshi, K., Endo, T., 2009. Uptake of phenoxyacetic acid derivatives into Caco-2 cells by the monocarboxylic acid transporters. Toxicol. Lett. 189, 102–109.

Kotaki, Y., Koike, K., Sato, S., Ogata, T., Fukuyo, Y., Kodama, M., 1999. Confirmation of domoic acid production of *Pseudo-nitzschia multiseries* isolated from Ofunato Bay, Japan. Toxicon 37, 677–682.

Lappin, G.J., Hardwick, T.D., Stow, R., Pigott, G.H., van Ravenzwaay, B., 2002. Absorption, metabolism and excretion of 4-chloro-2-methylphenoxyacetic acid (MCPA) in rat and dog. Xenobiotica 32, 153–163.

Lecona, E., Olmo, N., Turnay, J., Santiago-Gómez, A., López de Silanes, I., Gorospe, M., Lizarbe, M.A., 2008. Kinetic analysis of butyrate transport in human colon adenocarcinoma cells reveals two different carrier-mediated mechanisms. Biochem. J. 409, 311–320.

Lefebvre, K.A., Robertson, A., 2010. Domoic acid and human exposure risks: a review. Toxicon 56, 218–230.

Mordrelle, A., Huneau, J.F., Tomé, D., 1997. Sodium-dependent and -independent transport of L-glutamate in the rat intestinal crypt-like cell line IEC-17. Biochem. Biophys. Res. Commun. 233, 244–247.

Mordrelle, A., Jullian, E., Costa, C., Cormet-Boyaka, E., Benamouzig, R., Tomé, D., Huneau, J.F., 2000. EAAT1 is involved in transport of L-glutamate during differentiation of the Caco-2 cell line. Am. J. Physiol. Gastrointest. Liver Physiol. 279, G366–G373.

Nicklin, P.L., Irwin, W.J., Hassan, I.F., Mackay, M., Dixon, H.B.F., 1995. The transport of acidic amino acids and their analogues across monolayers of human intestinal absorptive (Caco-2) cells in vitro. Biochim. Biophys. Acta 1269, 176–186.

Ogihara, T., Tamai, I., Tsuji, A., 1999. Structural characterization of substrates for the anion exchange transporter in Caco-2 cells. J. Pharm. Sci. 88, 1217–1221.

Quilliam, M.A., Sim, P.G., McCulloch, A.W., McInnes, A.G., 1989. High-performance liquid chromatography of domoic acid, a marine neurotoxin, with application to shellfish and plankton. Int. J. Environ. Anal. Chem. 36, 139–154.

Rajendran, V.M., Harig, J.M., Adams, M.B., Ramaswamy, K., 1987. Transport of acidic amino acids by human jejunal brush-border membrane vesicles. Am. J. Physiol. 252, G33–G39.

Ross, I.A., Johnson, W., Sapienza, P.P., Kim, C.S., 2000. Effects of the seafood toxin domoic acid on glutamate uptake by rat astrocytes. Food Chem. Toxicol. 38, 1005–1011.

Sai, Y., Kaneko, Y., Ito, S., Mitsuoka, K., Kato, Y., Tamai, I., Artursson, P., Tsuji, A., 2006. Predominant contribution of organic anion transporting polypeptide OATP-B (OATP2B1) to apical uptake of estrone-3-sulfate by human intestinal Caco-2 cells. Drug Metab. Dispos. 34, 1423–1431.

Suzuki, C.A.M., Hierlihy, S.L., 1993. Renal clearance of domoic acid in the rat. Food Chem. Toxicol. 31, 701–706.

Truelove, J., Iverson, F., 1994. Serum domoic acid clearance and clinical observations in the cynomolgus monkey and Sprague-Dawley rat following a single i.v. dose. Bull. Environ. Contam. Toxicol. 52, 479–486.

Truelove, J., Mueller, R., Pulido, O., Iverson, F., 1996. Subchronic toxicity study of domoic acid in the rat. Food Chem. Toxicol. 34, 525–529.

Truelove, J., Mueller, R., Pulido, O., Martin, L., Fernie, S., Iverson, F., 1997. 30-day oral toxicity study of domoic acid in cynomolgus monkeys: lack of overt toxicity at doses approaching the acute toxic dose. Nat. Toxins 5, 111–114.

Tsuji, A., Tamai, I., 1996. Carrier-mediated intestinal of drugs. Pharm. Res. 13, 963–977.

Weerachayaphorn, J., Pajor, A.M., 2008. Identification of transport pathways for citric acid cycle intermediates in the human colon carcinoma cell line, Caco-2. Biochim. Biophys. Acta 1778, 1051–1059.

Wright, J.L.C., Boyd, R.K., de Freitas, A.S.W., Falk, M., Foxall, R.A., Jamieson, W.D., Laycock, M.V., McCulloch, A.W., McInnes, A.G., Odense, P., Pathak, V.P., Quilliam, M.A., Ragan, M.A., Sim, P.G., Thibault, P., Walter, J.A., Gilgan, M., Richard, D.J.A., Dewar, D., 1989. Identification of domoic acid, a neuroexcitatory amino acid, in toxic mussels from eastern Prince Edward Island. Can. J. Chem. 67, 481–490.

Solubility of Iron in the Aerosol Collected during Kosa (Asian Dust) Events in Japan

Ikuko Mori[1], Masataka Nishikawa[1], Atsushi Shimizu[1], Masamitsu Hayasaki[2], and Takumi Takasuga[3]
[1]*National Institute for Environmental Studies, Tsukuba, Japan*
[2]*Center for Environmental Remote Sensing, Chiba University, Chiba, Japan*
[3]*Shimadzu Techno-Research, Kyoto, Japan*

Abstract

The main contributor of aerosol particulate soluble iron to Japan and the Pacific Ocean has been investigated using data obtained during the research campaign entitled "A Study on Dust and Sand Storms" conducted by the Ministry of the Environment, Japan. The concentration of particulate soluble iron was not correlated to total iron concentration. Particulate iron solubility ranged from less than 1% to 6%. It was low when the air mass was dominated by kosa aerosols, and high when the air mass was dominated by pollutants. Durations for the kosa and pollution events over Jeju Island, Matsue, and the Pacific Ocean in April and May 2007 were estimated using a Chemical Weather Forecasting System (CFORS). The estimated durations of the pollution events at Jeju and Matsue were slightly shorter than those of the kosa events. The calculated duration of the pollution event over the Pacific Ocean was only three hours, much shorter than that of the kosa event. Kosa aerosols are the main contributor of soluble iron to the Pacific Ocean; however anthropogenic aerosols should not be discounted as contributors of soluble iron to an area off the coast of the Asian continent.

1. Introduction

Iron is essential for the growth of organisms and may limit phytoplankton primary production, especially in the remote ocean, and several studies on the solubility of atmospheric particulate iron have been conducted (Zhuang et al. 1992; Spokes et al. 1994; Fan et al. 2006). Previous studies considered the solubility of aerosol iron mainly from two aspects; differences in leaching processes and differences in the source of the iron. Laboratory studies suggested that iron solubility should be predictable in terms of the pH/solubility relationship (Spokes et al. 1994) and demonstrated that acidification by gaseous nitric acid led to an increase in water-soluble iron (Duvall et al. 2008). Meskhidze et al. (2003) predicted that the pH estimated by using the observed nitrate ion and gaseous nitric acid concentrations was low enough to facilitate iron mobilisation in mineral dust from East Asia. On the other hand, the laboratory study conducted by Schroth et al. (2009) showed that the solubility of iron in an aerosol could vary depending on its source; the measured solubility of iron in arid soils was less than 1%, that in glacially produced soils was 2−3%, whereas in oil combustion products it was 77−81%. Acid processing of insoluble iron was not significant in authentic aerosol samples (Chuang et al. 2005; Baker et al. 2006). Aguilar-Islas et al. (2010) concluded, based on the result of leaching experiments and using data from the literature, that more variability in aerosol iron solubility resulted from differences in aerosol type than from different leaching protocols.

The main contributing source of soluble iron, especially to the remote ocean, is still a matter of controversy. Chuang et al. (2005) concluded, based on the results of chemical analysis, that the iron released by fuel combustion was the main contributor of the soluble iron in aerosols collected in Jeju, Korea. Sedwick et al. (2007) agreed with this conclusion following chemical analysis of aerosols collected from the Sargasso Sea. A model calculation suggested that anthropogenic emissions contributed approximately 70% and 85% of the annual dry deposition of soluble iron to the surface ocean near Bermuda and Ireland, respectively (Sholkovitz et al. 2009). Another model calculation suggested that iron from combustion processes can represent up to 50% of the total iron deposited, but over open ocean regions it usually contributes less than 5% of the total iron, with the highest values (< 30%) close to the East Asian continent in the North Pacific (Luo et al. 2008).

In this paper, the main contributor of soluble iron to Japan and the Pacific Ocean was investgated using data obtained during the research initiative entitled "A study on Dust and Sand Storms" conducted by the Ministry of the Environment, Japan.

2. Aerosol samples and methods

Since 2002 the Ministry of the Environment of Japan has conducted a research campaign entitled "A Study on Dust and Sand Storms" to investigate the physical and chemical characteristics of kosa (Asian dust) aerosols. During this research, total suspended particulates (TSP) were collected in nine locations throughout Japan (Fig. 1) using high volume samplers with quartz fibre filters, when kosa events were observed in China.This aerosol sampling has been conducted a few times each year. The aerosol mass concentration and the concentrations of the chemical components of the aerosols were determined by the procedure described by Mori et al. (2002). In brief, water-soluble components were extracted using ultrapure water, and bulk components were digested using a mixture of nitric, perchloric, and hydrofluoric acids. Aerosol vertical distribution was measured by lidar (Shimizu et al. 2004). The concentrations of suspended particulate matter (SPM) and sulfur dioxide (SO_2) were measured simultaneously. Five events (Table 1) were selected for discussion of the characteristics of water soluble iron in aerosols collected during heavy dust events. Results of backward trajectory analyses revealed that the air masses came to Japan from the Asian continent during these events. Details of the research campaign and the selected heavy dust events are described in MOE (2009).

3. Results and discussion

3.1 Total and water soluble iron concentrations

Concentrations of TSP, total iron (Fe), and water soluble iron in the aerosols collected during five heavy dust events over Japan were in the ranges 66−509 μg m^{-3}, 1.7−20.2 μg m^{-3}, < 0.01−0.13 μg m^{-3}, respectively. The concentration of total iron increased with an increase in the TSP concentration. However, the concentration of water soluble iron did not increase with increases in TSP or total iron concentrations (Fig. 2). This result agreed with that from aerosol monitoring in Jeju Island, Korea (Chuang et al. 2005). The particulate soluble iron concentration is not correlated to the total iron concentration in the Asian outflow atmosphere.

Corresponding author: Ikuko Mori, National Institute for Environmental Study, 16-2 Onogawa, Tsukuba 305-8506, Japan. E-mail: mori.ikuko@nies.go.jp.

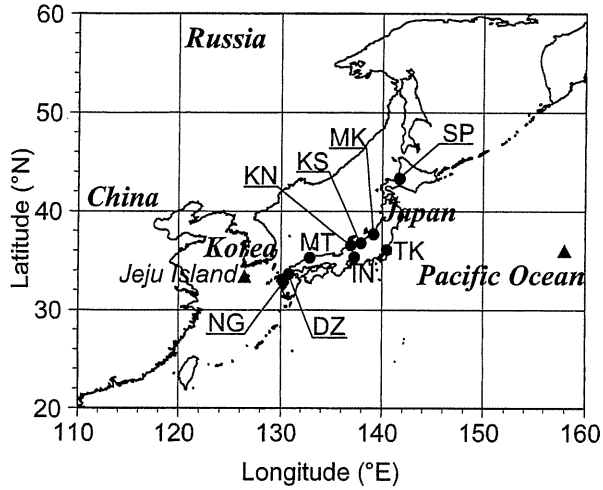

Fig. 1. TSP sampling locations (circles). DZ: Dazaifu, IN: Inuyama, KN: Kanazawa, KS: Kosugi, MK: Maki, MT: Matsue, NG: Nagasaki, SP: Sapporo, TK: Tsukuba. Locations selected for the CFORS calculation (Jeju Island and the Pacific Ocean) are also shown (triangles).

3.2 Particulate iron solubility and source

The particulate iron solubility ranged from less than 1% to 6% during the five heavy dust events in Japan. This result is consistent with that reported for the Jeju aerosol (Chuang et al. 2005; Duvall et al. 2008) and with that for the aerosol collected over the Sagrasso Sea (Sedwick et al. 2007).

Laboratory studies demonstrated that the solubility of iron in loess was less than 1% (Duvall et al. 2008; Schroth et al. 2009). In contrast, the solubility of iron in oil combustion products ranged from 49–100% (Henry and Knapp 1980; Schroth et al. 2009). These results derived from laboratory studies indicated that particulate iron solubility in aerosols could be controlled by the source of the aerosol.

To investigate the relationship between the solubility of particulate iron and the contribution of kosa to the aerosol, the particulate iron solubility was plotted against the ratio of the aluminium concentration to TSP (Fig. 3), which shows the particulate iron solubility decreased as the Al/TSP increased. Aluminium is often used as an indicator of mineral aerosols (Uematsu et al. 1983; Duce 1995), and therefore the higher the Al/TSP, the higher the contribution of kosa to the aerosol. That kosa was the main contributor to the aerosol was also supported by the observation that its Fe/Al value approached 0.5, very close to the Fe/Al value for Simulated Asian Mineral Dust certified reference material (0.51) (Nishikawa et al. 2000), as Al/TSP increased (Fig. 4). From these results, it could be concluded that the solubility of particulate iron was ca 1% when kosa aerosol was the predominant material in the atmosphere.

The particulate iron solubility was also plotted against the ratio of the sum of the concentrations nitrate (NO_3^-) and non-sea salt sulfate ($nssSO_4^{2-}$) ions (Anion) to TSP (Fig. 5) in order to investigate the relationship between iron solubility and the contribution of anthropogenic aerosol. Sulfate and nitrate ions are mainly formed from substances supplied to the atmosphere through human activity. Generally, a higher Anion/TSP value indicates a higher contribution of an anthropogenic aerosol. Figure 5 shows that the particulate iron solubility was high when the Anion/TSP was high. This result suggested that particulate iron solubility is high when anthropogenic aerosols are predominant in the atmosphere.

The dependency of particulate iron solubility on air mass type was also investigated. The air mass was categorised: 1) kosa, 2) kosa + pollutant, 3) pollutant; according to the analytical results of lidar measurements and SPM and SO_2 measurements (MOE

Table 1. Selected heavy dust event.

Event	Date	Note
1	8–9 April 2006	Kosa
2	18–19 April 2006	Kosa
3	1–2 April 2007	Kosa (TAD-2007*)
4	8–9 May 2007	Pollution**
5	26–27 May 2007	Kosa

*: Typical Asian Dust 2007
**: Hayasaki et al. (2008) and Ohara et al. (2008)

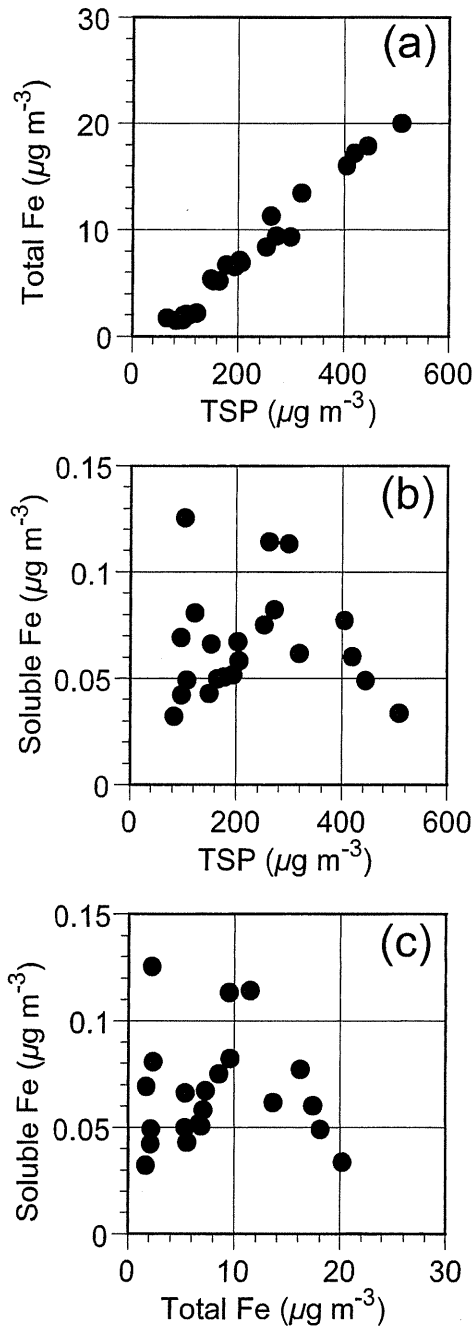

Fig. 2. The relationship between (a) particulate total Fe and TSP (b) particulate soluble Fe and TSP, and (c) particulate soluble Fe and total Fe concentration for the aerosols collected during heavy dust events in Japan.

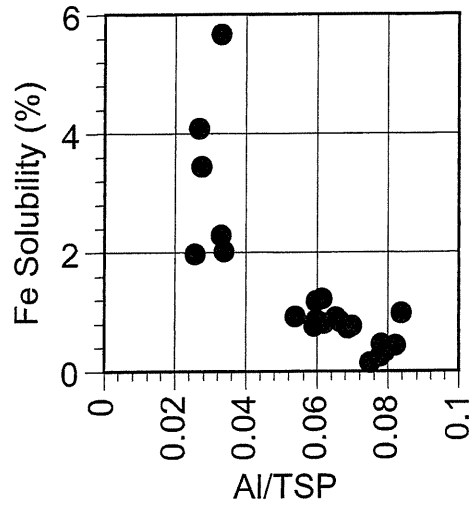

Fig. 3. The relationship between particulate iron solubility and Al/TSP for the aerosols collected during heavy dust events in Japan.

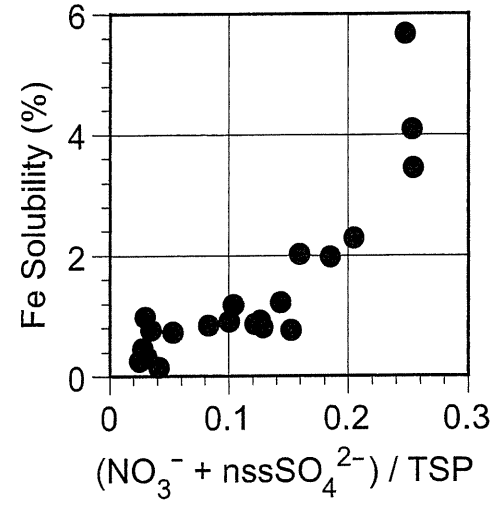

Fig. 5. The relationship between particulate iron solubility and (NO_3^- + $nssSO_4^{2-}$)/TSP for the aerosols collected during heavy dust events in Japan.

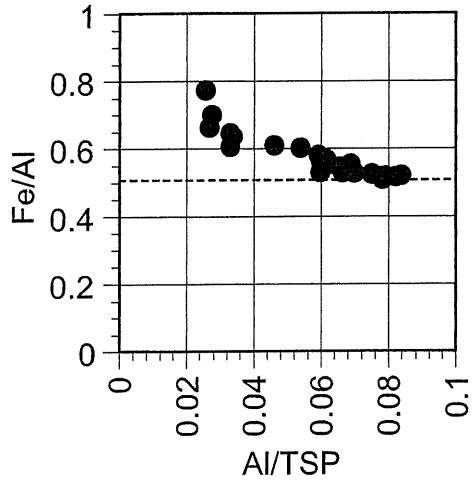

Fig. 4. The relationship between Fe/Al and Al/TSP for the aerosols collected during heavy dust events in Japan. The dotted line represents Fe/Al for Simulated Asian Mineral Dust certified reference material (CJ-2).

2009). The solubility of iron in the aerosol collected when the air mass was categorised as kosa was low, and the iron solubility when the air mass was categorised as pollutant was high (Table 2).

These results were consistent with the results of the laboratory study as described above. Particulate iron solubility in the atmosphere over Japan would be controlled by the aerosol source as described by Schroth et al. (2009) and Aguilar-Islas et al. (2010).

3.3 Primary contributor of particulate soluble iron to Japan and the Pacific Ocean

The soluble iron concentrations in the aerosols in each air mass category are summarised in Table 2. Differences in the soluble iron concentration in each air mass category were insignificant, although the differences in the iron solubility were significant. Therefore, iron solubility was not a key factor in controlling the amount of particulate soluble iron. The duration of each event (kosa, pollution or a combination of the two) would be the key factor in controlling the quantity of particulate soluble iron.

To estimate the duration of a kosa event and a pollution event, dust and sulfate concentrations throughout April and May 2007 were calculated using a chemical weather forecasting system (CFORS) (Uno et al. 2004). Three locations: 1) Jeju, Korea, 2) Matsue, Japan, 3) the Pacific Ocean (Fig. 1); were selected for this analysis. In this paper, when the calculated dust concentration near the surface exceeded 100 μg m^{-3} was categorised as the kosa event, and when the calculated sulfate concentration near the surface exceeded 10 μg m^{-3} was categorised as the pollution event. These threshold values were determined based upon CFORS results during kosa and pollution events observed in Matsue. The calculated total duration of the kosa event at Jeju and Matsue was slightly longer than that for the pollution event (Table 3). This suggested that a kosa event supplies more soluble iron to these locations than does a pollution event. This result contradicts that of Chuang et al. (2005) who concluded that soluble iron was mainly derived from anthropogenic activity with mineral dust making a negligible contribution. However, the calculated total duration of the pollution event over the Pacific Ocean was only three hours, and was much shorter than the kosa event (Table 3). This suggested that kosa aerosol is the main contributor of particulate soluble iron to the Pacific Ocean. This finding is consistent with that of Sholkovitz et al. (2009) that the annual mean dry deposition of

Table 2. Median and range (in parentheses) of TSP, particulate total iron, particulate soluble iron, and iron solubility for the aerosols collected during high TSP events in Japan. Air mass was categorised according to the results of lidar, SPM and SO_2 measurements.

Air mass	TSP (μg m^{-3})	Total Fe (μg m^{-3})	Soluble Fe (μg m^{-3})	Fe Solubility (%)
Kosa	404 (149–509)	16.2 (5.5–20.2)	0.061 (0.034–0.115)	0.46 (0.17–1.00)
Kosa + Pollutant	198 (66–298)	7.0 (1.9– 9.6)	0.063 (< 0.01–0.114)	0.88 (< 0.1–1.24)
Pollutant	100 (83–122)	2.1 (1.7– 2.4)	0.060 (0.033–0.126)	2.9 (2.0– 5.7)

Table 3. Estimated duration of the kosa and pollution events over Jeju Island, Matsue, and the Pacific Ocean by CFORS in April and May 2007.

(h)	Kosa	Pollution
Jeju Island, Korea	312	165
Matsue, Japan	315	255
Pacific Ocean	72	3

soluble iron at Barbados and Izana is dominated by soil dust, even though the study location was different. It is also consistent with the conclusions based on the Saharan dust study by Baker et al. (2006). We conclude that kosa aerosols are the main contributor of soluble iron to remote ocean, such as those of the Pacific Ocean, but that anthropogenic aerosols should not be discounted as sources of soluble iron area of sea off the coast of the Asian continent.

4. Summary

The following conclusions were derived from the results of the research campaign entitled "A Study on Dust and Sand Storms" conducted by the Ministry of the Environment, Japan:

1. The particulate soluble iron concentration in the Asian outflow atmosphere is not correlated to the total iron concentration.
2. The solubility of particulate iron in the atmosphere over Japan depends upon the source of the aerosol.
3. Kosa aerosols are the main contributor of soluble iron to the remote ocean, such as the Pacific Ocean, but anthropogenic aerosols should not be discounted as a source of soluble iron to areas off the coast of the Asian continent.

Acknowledgements

The authors thank the members of "A Study on Dust and Sand Storms" for collecting the aerosol samples and for various datasets. Part of this research was supported by the Environment Research and Technology Development Fund (B-0901) of the Ministry of the Environment, Japan. This paper contributes to research undertaken under the TEMM-WG1.

References

Aguilar-Islas, A. M., J. Wu, R. Rember, A. M. Johansen, and L. M. Shank, 2010: Dissolution of aerosol-derived iron in seawater: Leach solution chemistry, aerosol type, and colloidal iron fraction. *Marine Chem.*, **120**, 25–33.

Baker, A. R., T. D. Jickells, M. Witt, and K. L. Linge, 2006: Trends in the solubility of iron, aluminium, manganese and phosphorus in aerosol collected over the Atlantic Ocean. *Marine Chem.*, **98**, 43–58.

Chuang, P. Y., R. M. Duvall, M. M. Shafer, and J. J. Schauer, 2005: The origin of water soluble particulate iron in the Asian atmospheric outflow. *Geophys. Res. Lett.*, **32**, L07813, doi:10.129/2004GL021946.

Duce, R. A., 1995: Sources, distributions, and fluxes of mineral aerosols and their relationship to climate: in Aerosol Forcing of Climate, Wiley, 43–72 pp.

Duvall, R. M., B. J. Majestic, M. M. Shafer, P. Y. Chuang, B. R. T. Simoneit, and J. J. Schauer, 2008: The water-soluble fraction of carbon, sulfur, and crustal elements in Asian aerosols and Asian soils. *Atmos. Environ.*, **42**, 5872–5884.

Fan, S.-M., W. J. Moxim, and H. L. II, 2006: Aeolian input of bioavailable iron to the ocean. *Geophys. Res. Lett.*, **33**, L070602, doi:10.1029/2005GL024852.

Hayasaki, M., T. Ohara, J. Kurokawa, I. Uno, and A. Shimizu, 2008: Episodic pollution of photochemical ozone during 8-9 May 2007 over Japan: Observational data analyses. *J. Japan Soc. Atmos. Environ.*, **43**, 225–237.

Henry, W. M., and K. T. Knapp, 1980: Compound forms of fossil fuel fly ash emissions. *Environ. Sci. Technol.*, **14**, 450–456.

Luo, C., N. Mahowald, T. Bond, P. Y. Chuang, P. Artaxo, R. Siefert, Y. Chen, and J. Schauer, 2008: Combustion iron distribution and deposition. *Global Biogeochem. Cycles*, **22**, GB1012, doi:10.1029/2007GB002964.

Meskhidze, N., W. L. Chameides, A. Nenes, and G. Chen, 2003: iron mobilization in mineral dust: Can anthropogenic SO_2 emissions affect ocean productivity?. *Geophys. Res. Lett.*, **30**, 2085.

MOE, 2009: Ministry of the Environment, Japan Kosa jittai kaimei chosa hokokusyo, 169 pp.

Mori, I., M. Nishikawa, H. Quan, and M. Morita, 2002: Estimation of the concentration and chemical composition of kosa aerosols at their origin. *Atmos. Environ.*, **36**, 4569–4575.

Nishikawa, M., Q. Hao, and M. Morita, 2000: 0363 Preparation and evaluation of certified reference materials for Asian mineral dust. *Global Environ. Res.*, **4**, 103–113.

Ohara, T., I. Uno, J.-I. Kurokawa, M. Hayasaki, and A. Shimizu, 2008: Episodic pollution of photochemical ozone during 8–9 May 2007 over Japan –Overview–. *J. Japan Soc. Atmos. Environ.*, **43**, 198–208.

Schroth, A. W., J. Crusius, E. R. Sholkovitz, and B. C. Bostick, 2009: Iron solubility driven by speciation in dust sources to the ocean. *Nat. Geosci.*, **2**, 337–340.

Sedwick, P. N., E. R. Sholkovitz, and T. M. Church, 2007: Impact of anthropogenic combustion emissions on the fractional solubility of aerosol iron: Evidence from the Sargasso Sea. *Geochem. Geophys. Geosys.*, **8**, Q10Q06, doi:10.1029/2007GC001586.

Shimizu, A., N. Sugimoto, I. Matsui, K. Arao, I. Uno, T. Murayama, N. Kagawa, K. Aoki, A. Uchiyama, and A. Yamazaki, 2004: Continuous observations of Asian dust and other aeroosols by polarization lidars in China and Japan during ACE-Asia. *J. Geophys. Res.*, **109**, D19S17, doi:10.1029/2002JD003253.

Sholkovitz, E. R., P. N. Sedwick, and T. M. Church, 2009: Influence of anthropogenic combustion emissions on the deposition of soluble aerosol iron to the ocean: Empirical estimates for island sites in the North Atlantic. *Geochim. Cosmochim. Acta*, **73**, 3981–4003.

Spokes, L. J., T. D. Jickells, and B. Lim, 1994: Solubilisation of aerosol trace metals by cloud processing: A laboratory study. *Geochim. Cosmochim. Acta*, **58**, 3281–3287.

Uematsu, M., R. A. Duce, J. M. Prospero, L. Chen, J. T. Merrill, and R. L. McDonald, 1983: Transport of mineral aerosol from Asia over the North Pacific Ocean. *J. Geophys. Res.*, **88**, 5343–5352.

Uno, I., S. Satake, G. R. Carmichael, Y. Tang, Z. Wang, T. Takemura, N. Sugimoto, A. Shimizu, T. Murayama, T. A. Cahill, S. Cliff, M. Uematsu, S. Ohta, P. K. Quinn, and T. S. Bates, 2004: Numerical study of Asian dust transport during the springtime of 2001 simulated with the Chemical Weather Forcasting System (CFORS) model. *J. Geophys. Res.*, **109**, D19S24, doi:10.1029/2003JD004222, 2004.09.

Zhuang, G., Z. Yi, R. A. Duce, and P. R. Brown, 1992: Link between iron and sulphur cycles suggested by detection of Fe (II) in remote marine aerosols. *Nature*, **355**, 537–539.

Manuscript received 3 November 2010, accepted 22 December 2010
SOLA: http://www.jstage.jst.go.jp/browse/sola/

Harmful Algae 10 (2011) 456–462

Contents lists available at ScienceDirect

Harmful Algae

journal homepage: www.elsevier.com/locate/hal

Unique amnesic shellfish toxin composition found in the South East Asian diatom *Nitzschia navis-varingica*

Marc Lawrence J. Romero [a], Yuichi Kotaki [b,*], Nina Lundholm [c], Hikmah Thoha [d], Hisao Ogawa [b], Juan R. Relox [a], Ryuta Terada [e], Shigenobu Takeda [f], Yoshinobu Takata [b], Koichi Haraguchi [g], Tetsuya Endo [h], Po-Teen Lim [i], Masaaki Kodama [b], Yasuwo Fukuyo [j]

[a] *Bureau of Fisheries and Aquatic Resources, 860 Arcadia Building, Quezon Avenue, Quezon City 1100, Philippines*
[b] *School of Marine Biosciences, Kitasato University, Sanriku, Ofunato, Iwate 022-0101, Japan*
[c] *The Natural History Museum of Denmark, Soelvgade 83 Opg S, DK-1307 Kbh K, Denmark*
[d] *Center for Oceanographic Research-LIPI, Jl. Pasir Putih No. 1, Ancol Timur, Jakarta 11048, Indonesia*
[e] *Faculty of Fisheries, Kagoshima University, Shimoarata, Kagoshima 890-0056, Japan*
[f] *Faculty of Fisheries, Nagasaki University, Bunkyo, Nagasaki 852-8521, Japan*
[g] *Daiichi College of Pharmaceutical Sciences, Tamagawa, Minami, Fukuoka 815-8511, Japan*
[h] *Faculty of Pharmaceutical Sciences, Health Sciences University of Hokkaido, Tobetsu, Ishikari, Hokkaido 061-0293, Japan*
[i] *Faculty of Resource Science and Technology, University of Malaysia Sarawak, Kota Samarahan, Sarawak 94300, Malaysia*
[j] *Asian Natural Environmental Science Center, The University of Tokyo, Yayoi, Bunkyo, Tokyo 113-8657, Japan*

ARTICLE INFO

Article history:
Received 23 September 2010
Received in revised form 22 February 2011
Accepted 23 February 2011
Available online 1 March 2011

Keywords:
Amnesic shellfish poisoning
Domoic acid
Estuary
Isodomoic acid
Nitzschia navis-varingica
Pennate diatom

ABSTRACT

Nitzschia navis-varingica is a diatom that is known to produce significant levels of amnesic shellfish poisoning (ASP) toxins. A total of 33 *N. navis-varingica* strains were isolated from four brackish water localities in the Philippines and Indonesia, and cultured to characterize the toxins produced. The isolates were analyzed for domoic acid (DA) and isodomoic acids A (IA) and B (IB) by HPLC with fluorescence detection. Two toxin composition types were detected that have not been previously described: strains producing only IB and strains producing DA–IA–IB. These two types were isolated from two different localities. Eighteen strains were isolated from the Philippines (northern Luzon Island). Among them, 10 isolates from Alaminos produced only IB with an average toxin content of 3.05 pg cell^{-1}, seven isolates from Bulacan produced DA and IB with average toxin contents of 0.68 pg cell^{-1} and 1.18 pg cell^{-1}, respectively. One isolate from Cavite produced DA, IA, and IB with a toxin content of 0.58, 0.20, and 0.92 pg cell^{-1}, respectively. Fifteen isolates from Indonesia (Bone, South Sulawesi) produced only DA (four isolates) or DA with trace amounts of IB (eleven isolates), with an average toxin content of 2.38 pg cell^{-1} and 0.06 pg cell^{-1}, respectively. Sub-strains were established from strains producing either of the three toxin types: IB, DA–IA–IB, and DA-trace IB. Results showed that the toxin composition type was the same for parent and sub-strains, indicating that the toxin composition is a stable character for a strain.

1. Introduction

Domoic acid (DA) and its derivatives (e.g., isodomoic acids A, B, C, G, and H) (Maeda et al., 1986; Zaman et al., 1997) are insecticidal agents first isolated from the macro-alga *Chondria armata* (Takemoto & Daigo, 1958). Later, DA was identified as the toxin responsible for amnesic shellfish poisoning (ASP) (Wright et al., 1989) followed by identification of the isomers isodomoic acids D, E, and F as minor components (Wright et al., 1990), and the causative organism was traced and identified as the diatom *Pseudo-nitzschia multiseries* (Bates et al., 1989). A number of DA-producing *Pseudo-nitzschia* spp. have been found in subsequent searches primarily in temperate areas, although the toxin level varied widely (Garrison et al., 1992; Martin et al., 1990; Lundholm et al., 1994; Rhodes et al., 1996; Rhodes, 1998; Orsini et al., 2002). Among them, three *Pseudo-nitzschia* species (*P. multiseries*, *P. australis*, and *P. seriata*) are known to produce high levels of DA (Bates et al., 1989; Garrison et al., 1992; Lundholm et al., 1994; Rhodes et al., 1996).

During a more recent search for DA-producing diatoms in tropical waters, a major DA-producing benthic diatom was isolated from Vietnam (Kotaki et al., 2000). This organism was identified as a new species, *Nitzschia navis-varingica* (Lundholm and Moestrup, 2000; Bates, 2000). This species has also been isolated from brackish water areas in the Philippines and Japan (Kotaki et al., 2004). Recently, some of the Philippine strains of *N. navis-varingica*

* Corresponding author. Tel.: +81 192 44 2121; fax: +81 192 44 2125.
E-mail address: kotaki@kitasato-u.ac.jp (Y. Kotaki).

1568-9883/$ – see front matter © 2011 Elsevier B.V. All rights reserved.
doi:10.1016/j.hal.2011.02.006

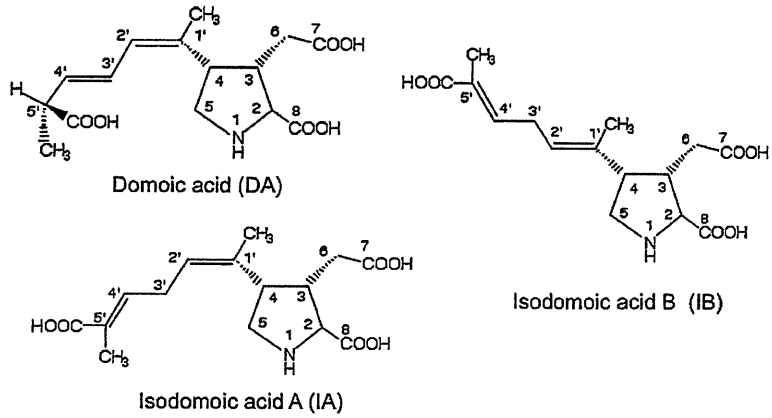

Fig. 1. Structure of domoic acid and isodomoic acids A and B.

were found to produce not only DA but also isodomoic acids A (IA) and B (IB) as major toxin components (Kotaki et al., 2005) (Fig. 1). ASP toxin production was then re-investigated using the strains of *N. navis-varingica* from the Philippines and a few other Asian countries (Japan, Vietnam, and Thailand) and three types of ASP toxin composition (DA, DA–IB, IA–IB) were detected. The most abundant toxin composition type was a combination of DA and IB (DA–IB), with the ratio of IB ranging from trace to ca. 80%. This type was found in strains from Japan, Thailand, Vietnam, and the Philippines (Kotaki, 2008; Kotaki et al., 2008; Romero et al., 2008). Isolates from restricted areas in the northern part of the Philippines had another toxin composition (IA and IB) (Bajarias et al., 2006; Kotaki, 2008; Kotaki et al., 2008). However, the composition and geographical distribution of toxins from southernmost Asia, such as Indonesia and Malaysia, and most of the northern part of the Philippines have not been studied.

We report here the results of a toxin screening of 33 *N. navis-varingica* strains from South Sulawesi in Indonesia and three localities in the Philippines. We document two new toxin composition types (IB and DA–IA–IB) from two different localities in the Philippines, although IA and IB might not pose a major health risk because of their lower toxicity than DA (Munday et al., 2008).

2. Materials and methods

2.1. Isolation and identification of N. navis-varingica

Samples were collected from the surface of mangrove roots or palm tree leaves hanging down into the water in estuarine areas using a handy scoop net (20 μm). Sampling was conducted in three areas of Luzon Island, Philippines, including several brackish sites, in December 2007 and December 2008: Alaminos in Pangasinan, and Bulacan and Cavite in Manila Bay (Fig. 2). Sampling was also conducted in several other brackish sites: Panyula, Bone in South Sulawesi (July 2008), Jakarta Bay (March 2009), Lampung Bay (March 2009), and Sangihe Island (May 2009), all in Indonesia, and finally in Kota Kinabalu, Malaysia (May 2008) (Fig. 2).

Crude cultures were prepared by mixing aliquots (0.2 mL or 1.0 mL) of net sample with 30 mL of f/2 medium in 50 mL tissue culture flasks (Greiner bio-one, Tokyo, Japan), and incubating them at 25 °C under an irradiance level of 60 μmol photons m^{-2} s^{-1} with a 16:8 h light:dark cycle. f/2 medium was prepared (Guillard, 1983) using sea water diluted with distilled water to a salinity of ca. 27 psu. Uni-algal cultures of *N. navis-varingica* were established from crude cultures by capillary washing of single cells under a light microscope (LM) according to the morphological characteristics of *N. navis-varingica* (Lundholm and Moestrup, 2000; Kotaki et al., 2005). The cells possess two yellow-brown chloroplasts at each end of the cell and are lanceolate in valve view. Cells are 38–110 μm long and 9–11 μm wide. In girdle view, the cells are rectangular and slightly indented at the middle. Most cells form ribbon-shaped colonies while growing (Kotaki et al., 2004). Experience have shown, that using these light microscopical characters allow us to isolate strains that have a high likelihood of being *N. navis-varingica*. One representative strain from each collection site was further investigated morphologically to confirm the identification using transmission electron microscopy (TEM) according to the method of Lundholm and Moestrup (2000). Subsamples were fixed in formalin (final concentration 3.7%). Representative strains identified using TEM were PBULD 07-4 (Bulacan, Manila Bay), PCAVA 07-2 (Cavite, Manila Bay), PALMC 07-1 (Alaminos, Pangasinan) (all from the Philippines), and IBNA 08-3, IBNB 08-4, and IBNC 08-3 (Panyula, Bone in South Sulawesi, all from Indonesia).

2.2. Analysis of ASP toxins in N. navis-varingica cultures

Isolates were cultured in 30 mL f/2 medium in 50 mL tissue culture tubes under the same culture conditions described in Section 2.1. The cultures were harvested after a 3-week culture period (mid-stationary growth phase). A 3 mL aliquot of whole culture was retrieved, boiled for 5 min and then centrifuged after being cooled to room temperature (Bajarias et al., 2006). A 2 mL aliquot was also retrieved for determining the cell density (Kotaki et al., 2000). Toxin profile analysis was done for DA, IA, and IB using HPLC-fluorescence analysis with pre-column derivatization using

Fig. 2. Sampling areas in the Philippines, Indonesia, and Malaysia.

9-fluorenylmethylchloroformate (FMOC-Cl) according to the slightly modified method of Pocklington et al. (1990) in which a Develosil ODS-5 column (4.6 × 250 mm, Nomura, Seto, Aichi, Japan) and a mobile phase of 40% acetonitrile in 20 mM phosphate buffer (pH 2.5) was used. The cellular toxin content was expressed on a per cell basis (pg cell^{-1}), which is calculated by dividing the total amount of each toxin (ng mL^{-1}) in the entire culture by the corresponding density of cells in the culture. The number of cells was determined using 5 μL of culture under LM in a Sedgewick-Rafter counting chamber. Samples were counted in triplicate and the average cell number was used for the cellular toxin content calculation. Standard toxins were purified from a mass culture of *N. navis-varingica* that produces both IA and IB (for IA and IB standards) and an extract of the red alga *C. armata* that produces high amount of DA and small/trace amount of IA, IB, 5′-epi-DA, etc. (for DA standard) collected in Kagoshima Prefecture, Japan. These were calibrated using commercial Canadian standard toxin (DACS-1D, DA) or purified toxins (IA and IB) (Kotaki et al., 2005).

Confirmation of toxin production of the representative strains was performed by LC–MS/MS using multiple reaction monitoring (MRM) (Takata et al., 2009). A 1 L mass culture of each strain was filtered (mixed cellulose ester 3 μm pore size filters, Advantec, Tokyo, Japan) at the end of the three-week culture period and the cells were extracted by boiling followed by ultrafiltration (10,000 Da cut-off). LC–MS was performed on an HP1100 LC system (Agilent Technologies, Santa Clara, CA) coupled to an Applied Biosystems/MDS Sciex API 2000 triple quadruple mass spectrometer (Applied Biosystems, Foster City, CA). LC separation was performed using a slight modification of the method described in the Canadian standard DACS-1D manual. A Wakosil Navi C18-5 column (2 mm × 250 mm; Wako, Tokyo, Japan) was employed, and analytes were eluted over 20 min using a linear gradient from 10% acetonitrile in 0.1% formic acid to 20% acetonitrile in 0.1% formic acid with a flow rate of 0.2 mL min^{-1}. The MS analysis was achieved by MRM with a turboion-spray interface in positive ion mode. Three MRM transitions from the protonated DA ion were monitored (*m/z* 312–266, *m/z* 312–248, and *m/z* 312–161). Standard toxin was prepared from an extract of *C. armata* and calibrated using commercial Canadian standard toxin (DACS-1D) or purified toxins (IA and IB) (Kotaki et al., 2005).

2.3. Toxin composition of *N. navis-varingica* sub-strains

Sub-strains were prepared by capillary washing of single cells of two representative parental Philippine strains: PALMC 07-1 (Alaminos, IB type), PCAVA 07-2 (Cavite, DA–IA–IB type), and one Indonesian parental strain: IBNB 08-2 (Panyula, Bone, DA-trace IB type), after having been pre-cultured for one week under the same conditions as the batch cultures in Section 2.1. Sub-strains were cultured for three weeks as described in Section 2.1, harvested and analyzed for toxin production as described in Section 2.2. The toxin composition was then compared with that of the parental strain. Parental strains were maintained for more than half year by inoculating aliquots of old culture into new f/2 medium every month followed by culturing for one week under the same conditions in Section 2.1.

3. Results

3.1. Isolation and identification of *N. navis-varingica*

Ten isolates of *N. navis-varingica* were obtained from Alaminos (PALM 07/08 strains, one in 2007 and nine in 2008), seven were

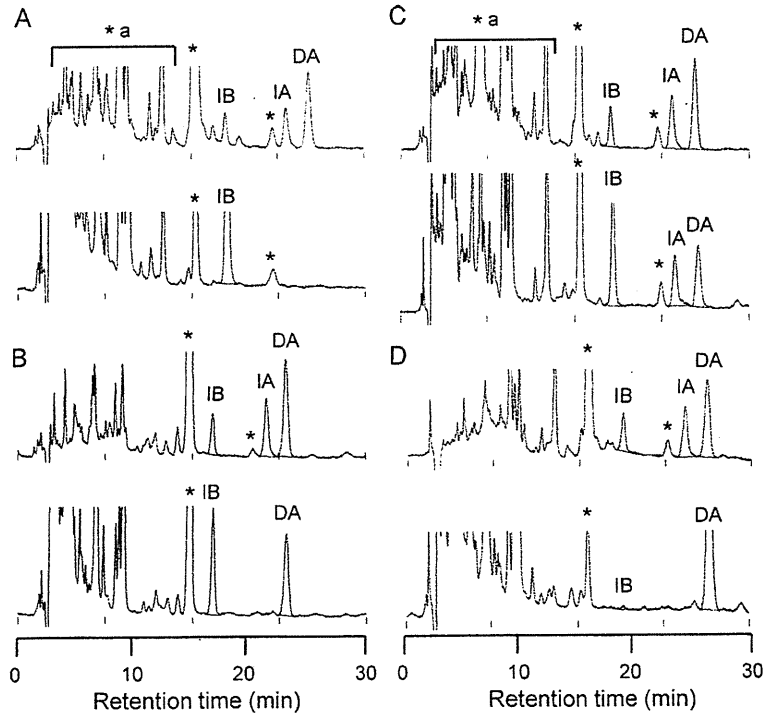

Fig. 3. HPLC-fluorescence analyses of ASP toxins from representative *Nitzschia navis-varingica* strains. Upper chromatogram of (A), (B), (C) and (D); standard toxins DAKS 04-1 containing IA, IB and DA (8.7, 9.2, and 17.5 ng/mL) analyzed at the same time as the respective sample. Lower chromatogram of (A), (B), (C) and (D); sample extracts of (A) PALMC 08-1 strain isolated from Alaminos, Pangasinan, (B) PBULD 07-5 isolated from Bulacan, Manila Bay, (C) PCAVA 07-2 isolated from Cavite, Manila Bay, all in the Luzon Island, the Philippines and (D) IBNB 08-3 isolated from Panyula, Bone, South Sulawesi, Indonesia. DA, domoic acid; IA, isodomoic acid A; IB, isodomoic acid B. *Side-products derived from the FMOC-Cl reagent. The amount of each derivative often varies due to contamination with compounds (e.g., other amino acids) that compete with ASP toxins and/or due to reaction conditions (Pocklington et al., 1990), *a: Side-products and/or reaction products derived from contaminants in the medium and other compounds in the culture (e.g., neutral amino acids) that react with the FMOC-Cl reagent. Analytical conditions: Develosil ODS-5 column (4.6 mm × 250 mm, Nomura); mobile phase, 40% acetonitrile in 20 mM phosphate buffer (pH 2.5); column temperature, 55 °C; flow rate, 1 mL min^{-1}; fluorescence detection, Ex. = 264 nm, Em. = 313 nm.

obtained from Bulacan (PBULD 08 strains), and one from Cavite (PCAVA 07 strain), all from the Philippines (Fig. 2). Fifteen strains of *N. navis-varingica* were obtained from Panyula, Bone, South Sulawesi, Indonesia (IBN 08 strain). No strains of *N. navis-varingica* were isolated from Jakarta Bay, Lampung Bay and Sangihe Island, all in Indonesia, or from Kota Kinabalu, in Malaysia (Fig. 2).

Morphological TEM studies of the strains PALMC 07-1 (Alaminos, Pangasinan), PBULD 07-4 (Bulacan, Manila Bay), PCAVA 07-2 (Cavite, Manila Bay) (all from the Philippines), and IBNA 08-3, IBNB 08-4, IBNC 08-3 (Panyula, Bone, all from Indonesia) that were positive for ASP toxin production agreed with Lundholm and Moestrup's (2000) description of *N. navis-varingica*. Characteristic silica ridges were observed in the wall of the raphe canal and on the mantle. The girdle bands were ornamented by silica warts and the valvocopula had 1–3 rows of poroids. On the valve, the density of interstriae was 25–28 in 10 μm, and the poroids in the uniseriate striae had a density of 3–5 poroids in 1 μm. The raphe was interrupted in the middle by a central interspace and the fibulae that did not show a central larger interspace had a density of 8–11 in 10 μm. The density of the poroids on the girdle bands was 32–42 in 10 μm.

3.2. ASP toxin production in N. navis-varingica cultures

Representative HPLC chromatograms and the average toxin composition of each strain positive for ASP production are shown in Figs. 3 and 4. Ten isolates from Alaminos, Pangasinan, the Philippines (PALM 07/08 strains) showed a new toxin composition type consisting only of IB. The isolates had an average toxin content of 3.05 pg cell^{-1} (σ = 3.65) (Fig. 3A, lower chromatogram). All seven isolates from Bulacan, Manila Bay, the Philippines (PBUL 07 strains) had the typical DA–IB toxin composition similar to that of strains isolated from the southern Philippines (Kotaki et al., 2005, 2008; Kotaki, 2008). The average content of DA and IB in the toxin across all strains was 0.68 pg cell^{-1} (σ = 0.35) and 1.18 pg cell^{-1} (σ = 0.46), respectively (1.86 pg cell^{-1} in total), and the DA:IB ratio was 37:63 (Fig. 3B, lower chromatogram). The strain isolated from Cavite, Manila Bay, the Philippines (PCAVA 07) had a new toxin composition type containing all three toxins (DA–IA–IB). The total toxin content for this strain was 1.70 pg cell^{-1} (DA, IA, and IB toxin content: 0.58, 0.20, and 0.92 pg cell^{-1}, with a DA:IA:IB ratio of 33:14:53) (Fig. 3C, lower chromatogram). The toxins produced by the 15 strains from Panyula, Bone, South Sulawesi, Indonesia consisted either of DA (4 strains) or DA-trace IB (11 strains). The average DA and IB toxin content across all the strains was 2.38 pg cell^{-1} (σ = 1.13) and 0.06 pg cell^{-1} (σ = 0.06), respectively (2.44 pg cell^{-1} in total), and the DA:IB ratio was 98:2 (Fig. 3D, lower chromatogram).

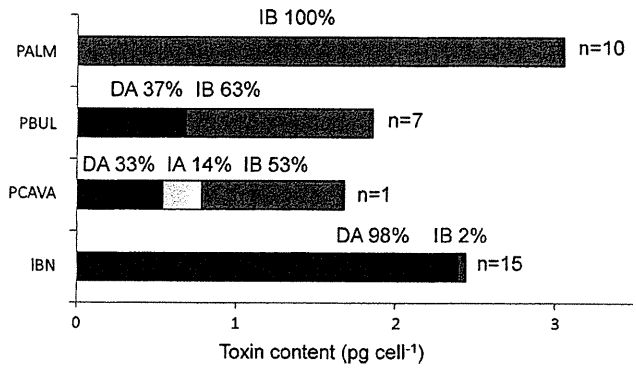

Fig. 4. Toxin composition of *Nitzschia navis-varingica* isolated from Luzon Island, Philippines and South Sulawesi, Indonesia. Black, domoic acid (DA); white, isodomoic aid A (IA); grey, isodomoic acid B (IB). Strains tested: PALM (Alaminos, Pangasinan, Philippines, One isolate in 2007 and 9 isolates in 2008), PBUL (Bulacan, Manila, Philippines, 2007), PCAVA (Cavite, Manila, Philippines, 2007), IBN (Panyula, Bone, South Sulawesi, Indonesia, 2008).

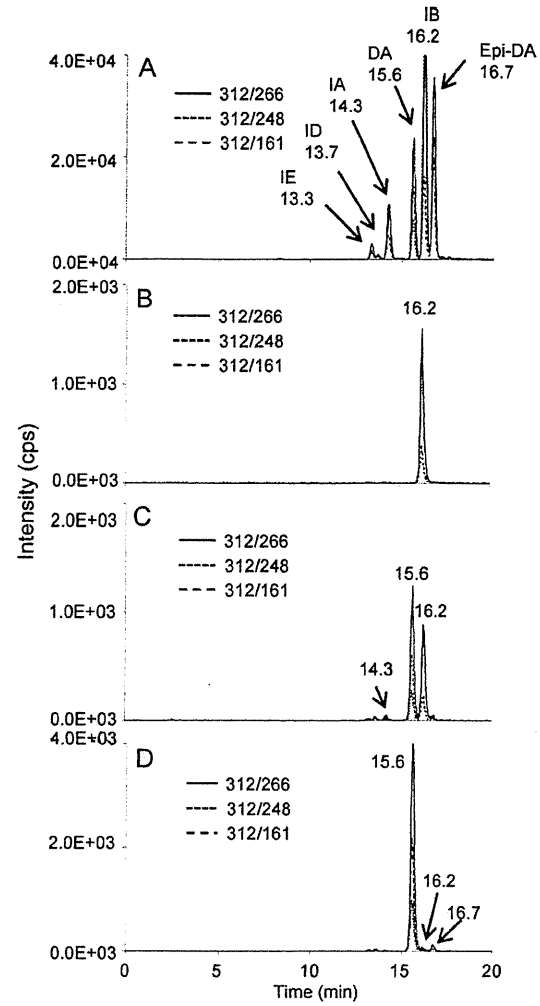

Fig. 5. Selected ion monitoring LC–MS/MS chromatogram of domoic acid and its isomers. Three MRM transitions from protonated DA were monitored (*m/z* 312–266, *m/z* 312–248, and *m/z* 312–161). DA, domoic acid; IA, isodomoic acid A; IB, isodomoic acid B. Standard toxins purified from *Chondria armata* followed by calibration with Canadian standard (DACS-1D) and isodomoic acids A and B purified from *Nitzschia navis-varingica* (Kotaki et al., 2005). (B) MRM chromatogram of toxin from *N. navis-varingica* strain PALMC 08-1 isolated from Alaminos, Pangasinan, the Philippines. (C) MRM chromatogram of toxin from *N. navis-varingica* strain PCAVA 07-2 isolated from Cavite, Manila Bay, the Philippines. (D) MRM chromatogram of toxin from *N. navis-varingica* strain IBNB 08-2 isolated from Panyula, Bone, South Sulawesi, Indonesia.

As shown in Fig. 5, the major toxin types produced by representative strains were confirmed by LC–MS/MS using multiple reaction monitoring (MRM) and comparing the results with LC chromatograms of standard toxins (Fig. 5A). Production of the following toxins was confirmed: (1) only IB was produced by a strain from Alaminos, the Philippines (PALMC 08-1 strain, Fig. 5B), (2) DA, IA, IB were produced by a strain isolated from Cavite, the Philippines (PCAVA 07-2 strain, Fig. 5C), and (3) DA and IB were produced by the strain isolated from Panyula, Bone, South Sulawesi Island, Indonesia (IBNB 08-2 strain, Fig. 5D).

3.3. Toxin composition of the N. navis-varingica sub-strains

Results of toxin composition analyses of the sub-strains are shown in Fig. 6 together with those of the corresponding parent. Thirty-three sub-strains were established from the IB type Philippine parental strain (PALMC 07-1 strain) with the IB toxin content of 4.59 pg cell^{-1}. All sub-strains had the same IB type toxin

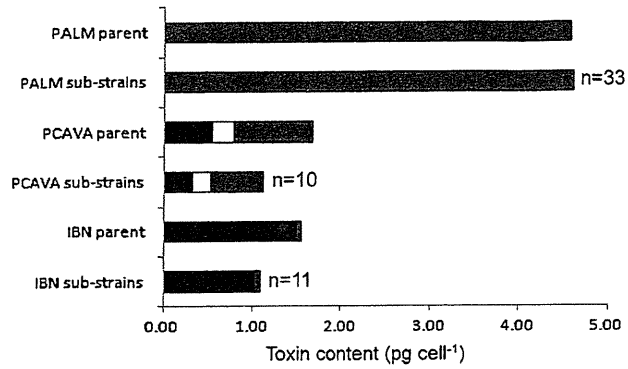

Fig. 6. Toxin composition of the sub-strains of *Nitzschia navis-varingica* compared with the respective parental strain. Black, domoic acid (DA); white, isodomoic aid (IA); grey, isodomoic acid B (IB). Parental strains used: PALM 07-1 (Alaminos, Pangasinan, Philippines, 2007), PCAV 07-2 (Cavite, Manila, Philippines, 2007), IBN 08-2 (Bone, South Sulawesi, Indonesia, 2008).

composition. The toxin composition was 100% IB with an average toxin content of 4.63 pg cell^{-1} (σ = 1.28), entirely lacking IA and DA (Fig. 6). Ten sub-strains were established from the DA–IA–IB type Philippine parental strain (PCAVA 07-2 strain) which had a total toxin content of 1.70 pg cell^{-1} with a DA:IA:IB toxin ratio of 33:14:53. The toxin in all the sub-strains was composed of DA–IA–IB, similar to the parental strain, with an average toxin content of 0.33 pg cell^{-1} (σ = 0.30), 0.19 pg cell^{-1} (σ = 0.15), and 0.60 pg cell^{-1} (σ = 0.45), respectively, and with a DA:IA:IB toxin ratio of 29:17:54 (Fig. 6). Eleven sub-strains were established from the Indonesian parental strain having a DA–IB type toxin composition (IBNB 08-2 strain) showing the total toxin content of 1.55 pg cell^{-1} with a DA:IB toxin ratio of 96:4. All sub-strains had the same toxin composition as the parental strain (DA–IB). The average DA and IB toxin content was 1.09 pg cell^{-1} (σ = 0.64) and 0.07 pg cell^{-1} (σ = 0.02), respectively, with an average DA:IB ratio of 94:6 (Fig. 6).

4. Discussion

We confirmed that *N. navis-varingica* can be found in estuarine areas of the northern part of Luzon Island, the Philippines and in South Sulawesi, Indonesia (Fig. 2). Interestingly, all 10 strains isolated from Alaminos, Luzon Island had a toxin composition only of IB without even trace amounts of any other isomers. The single isolate from Cavite, Luzon Island had the toxin content composed of DA–IA–IB. Neither of these two toxin composition types has been detected before in any diatom as major toxin components, and is described for the first time in the present study. Other isolates from Bulacan, Luzon Island, the Philippines and Bone, South Sulawesi, Indonesia showed the major toxin composition of DA–IB (including only DA) similar to *N. navis-varingica* from areas other than Luzon Island (Kotaki et al., 2005, 2008; Bajarias et al., 2006; Kotaki, 2008). Though total toxin content of each isolate had rather high variability, toxin composition was the same within each toxin composition type. The variability might come from a difference of culture conditions (e.g. difference of co-existing bacteria, difference of light intensity due to the location of tissue culture tube, etc.).

In this study, *N. navis-varingica* samples were collected mainly in dry season. It is thus unknown whether there is a seasonal difference in the distribution and toxin compositions of *N. navis-varingica*. Furthermore, we have not explored the possibility of other benthic diatoms producing ASP toxins. However, in Sakari Estuary, near our college, in Japan, *N. navis-varingica* could be isolated throughout the year (even in winter season, data not shown), all strains showing the same toxin composition (DA–IB). Our data indicate that *N. navis-varingica* might show the same toxin composition during all seasons in tropical areas. Detailed studies in different seasons at the same locality will be needed to further explore the seasonality of the distribution and toxin composition of *N. navis-varingica* in tropical areas.

Toxin compositions of *N. navis-varingica* isolates are summarized in Fig. 7 together with previously published results (Kotaki et al., 2005, 2008; Bajarias et al., 2006; Romero et al., 2008; Kotaki, 2008). The strains isolated from Panyula, Bone, South Sulawesi, Indonesia showed a DA-trace IB toxin composition type that was similar to those of strains isolated from Northern Japan (Kotaki et al., 2008; Kotaki, 2008) and Thailand (Romero et al., 2008), in contrast to the typical DA–IB type strains from Okinawa, southernmost Japan, strains from Vietnam, and some strains from the southern Philippines which had a higher proportion of IB (more than ca. 20%) (Kotaki et al., 2005, 2008; Kotaki, 2008). Our results show that toxin composition is not related to latitude, in contrary to what has previously been suggested, namely that the proportion

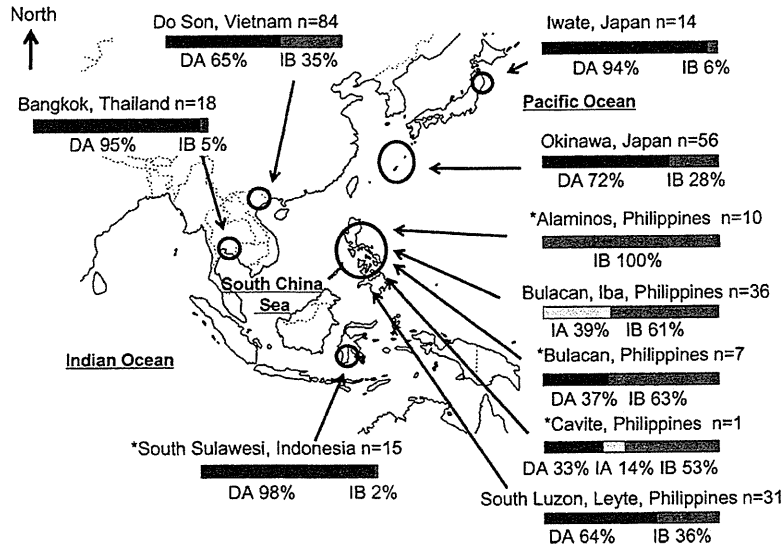

Fig. 7. Distribution and toxin composition of *Nitzschia navis-varingica* in Asian waters. Summary of the present studies and Kotaki et al. (2005, 2008), Bajarias et al. (2006), Romero et al. (2008) and Kotaki (2008). Black, domoic acid (DA); white, isodomoic acid A (IA); grey, isodomoic acid B (IB). *The present study.

of IB in the DA–IB type toxin should be higher in lower latitudes (Kotaki et al., 2005, 2008; Kotaki, 2008).

Sub-strains were established from strains representative of three different toxin composition types (IB, DA–IA–IB, and DA-trace IB), followed by toxin analysis. All of the sub-strains had the same toxin composition as the parental strains. As the parental strains were maintained for more than half year until use, above results demonstrate that toxin composition is most likely a stable character, although the exact ratio of each toxin component varies within each toxin composition type (Fig. 6). The stability of the character is also supported by supplemental batch culture experiments that were done using PALMC 07-1 (IB type) and PCAVA 07-2 (DA–IA–IB type) strains for up to 36 days resulting in confirmation that they maintained the same toxin profile type during the entire experimental period (PALMC strain; toxin content of IB increased up to 4.3 pg cell^{-1} at 36 day and PCAVA strain; total toxin content of DA–IA–IB showed maximum of 5.0 pg cell^{-1} at 28 day with the DA:IA:IB ratio of 37:14:49 and decreased to 4.2 pg cell^{-1} at 36 day with the DA:IA:IB ratio of 34:13:53).

As shown in Fig. 6, toxin content per cell between parent and sub-strain of PALMC 07-1 was almost the same (ca. 4.6 pg cell^{-1}) but in case of PCAVA 07-2 (DA–IA–IB type) and IBNB 08-3 (DA–IB type), average toxin content per cell of the sub-strains was a little lower than those of the parents. However, these differences are included in the variability of sub-strains (PCAVA; $\sigma = 0.87$, IBN; $\sigma = 0.66$).

Trace amounts of other isomers (e.g., isodomoic acids D and E together with DA, IA, and IB in the PCAVA 07 strain (Fig. 5C) and 5′-epi-DA together with DA and IB in the IBNB 08-2 strain (Fig. 5D) were detected in LC–MS/MS chromatograms of toxins from representative strains. However, the presence of these additional minor isomers was not confirmed in HPLC chromatograms with fluorescence detection because of low concentrations using an analysis method to extract samples without concentration (Pocklington et al., 1990; Kotaki et al., 2004). It is uncertain whether these minor isomers were artifacts produced by UV or heating (Wright et al., 1990; Quilliam, 2003) or whether they were bio-synthesized. Nevertheless, we did confirm that DA, IA, and IB are the major components of *N. navis-varingica* toxin, and that the toxin composition is more complex than previously reported (Kotaki et al., 2005, 2006; Bajarias et al., 2006; Kotaki, 2008). The presence of isodomoic acid C (IC) simultaneously with DA was recently reported in toxin of *P. australis* and shellfish that have fed on *P. australis* (Holland et al., 2003, 2005; Rhodes et al., 2003). We did not determine whether IC was present in this study due to a lack of standard toxin for comparison. However, it is unlikely that IC constitutes a major component of the toxin profile because no other apparent peak was observed in any of the HPLC and LC–MS/MS chromatograms.

Interestingly, only *N. navis-varingica* isolates from northern Luzon Island had a toxin composition different from the major DA–IB type. In total, three different toxin profiles have been confirmed in isolates from Luzon Island: IA–IB (Kotaki et al., 2005, 2008; Bajarias et al., 2006), IB, and DA–IA–IB (present study) (Fig. 7). The strains are morphologically similar to those found in other/close localities (Haiphong in Vietnam, Okinawa in Japan, the southern Philippines and Bulacan Estuary, Manila Bay in the Philippines).

One of the strains showing DA–IB toxin composition has been shown to change its toxin composition to the IA–IB type when grown in axenic culture and it returned to the original DA–IB type when the culture medium was replaced with the cell-free but non-axenic medium of the parental strain (Kotaki et al., 2008). This suggests that bacteria might play a role in controlling the toxin composition, but the mechanism is presently unknown. One possibility is that some kinds of bacteria might enhance DA production and/or block IA production and/or consume IA. Such bacteria might be absent at sites from which strains having a toxin composition that includes IA were isolated. Five types of ASP toxin compositions have been identified to date, namely DA, DA–IB, IA–IB, IB, and DA–IA–IB, although the difference between DA and DA–IB is uncertain because the ratio of IB varies (Fig. 7).

For the primary screening of ASP toxin-producing *N. navis-varingica*, the culture conditions described in Section 2.1 were used. The conditions are considered to be sufficiently similar to those of the seawater from which these *N. navis-varingica* strains were isolated. Temperature and salinity appear to not affect the toxin composition based on preliminary experiments (data not shown), but systematic examination of the factors affecting the toxin composition of this diatom, including co-existing bacteria, is needed. The detailed processes of the production of each toxin component are being investigated for determining the toxin production mechanism.

The toxicity of IA, IB, and IC is reported to be significantly lower than DA alone (Munday et al., 2008), suggesting that these toxins pose a lower risk to humans. However, the structural difference of DA and IB is based on the position of only one double bond: 3′–4′ (DA) and 4′–5′ (IA), and in IA and IB, the difference is due to only the configuration of Z (IA) and E (IB) at the 1′–2′ double bond (Fig. 1). Because of the structural similarities, there is a possibility that marine animals such as shellfish, fish and mammals may act as vectors of the toxin isomers, which might then be converted from IB to IA and finally to DA in the animal tissue, although there is no report showing these bioconversions in the animal tissue. Studies of such conversions are currently ongoing.

In conclusion, we isolated ASP toxin-producing diatom *N. navis-varingica* from selected areas of Luzon Island, the Philippines and South Sulawesi, Indonesia. Two new toxin composition types: (1) only IB and (2) DA, IA and IB were confirmed in the *N. navis-varingica* isolates from Luzon Island, the Philippines. The stability of these toxin compositions was confirmed by comparing the toxin composition of a parental strain and respective sub-strains. We summarized, in total, five ASP toxin composition types in *N. navis-varingica*. Investigation of factors affecting the toxin composition of *N. navis-varingica* might help in determining the toxin production mechanism of diatoms.

Acknowledgements

This work was supported in part by a grant-in-aid for research (C) from the Japan Society for the Promotion of Sciences (JSPS) and by a grant-in-aid for a multilateral cooperative research project (coastal oceanography), from the Ministry of Education, Science, Sports and Culture of Japan. We also thank Ms. Logen F. Enriquez of BFAR Region I Lucap, Alaminos, Pangasinan, for help in sample collection.

References

Bajarias, t.l., Kotaki Jr., F.F.A.Y., Romero, J.R.R., Furio, M.L.J., Lundholm, E.F., Koike, N., Fukuyo, K., Kodama, Y.M., 2006. Screening of diatoms producing domoic acid and its derivatives in the Philippines. Coast. Mar. Sci. 30, 121–129.

Bates, S.S., 2000. Domoic acid-producing diatoms: another genus added. J. Phycol. 36, 978–985.

Bates, S.S., Bird, C.J., deFreitas, A.S.W., Foxall, R., Gilgan, M., Hanic, L.A., Johnson, G.R., McCulloch, A.W., Odense, P., Pocklington, R., Quilliam, M.A., Sim, P.G., Smith, J.C., SubbaRao, D.V., Todd, E.C.D., Walter, J.A., Wright, J.L.C., 1989. Pennate diatom *Nitzschia pungens* as the primary source of domoic acid, a toxin in shellfish from eastern Prince Edward Island, Canada. Can. J. Fish. Aquat. Sci. 46, 1203–1215.

Garrison, D.L., Conrad, S.M., Eilers, P.P., Waldron, E.M., 1992. Confirmation of domoic acid production by *Pseudonitzschia australis* (Bacillariophyceae) cultures. J. Phycol. 28, 604–607.

Guillard, R.R.L., 1983. Culture of phytoplankton for feeding marine invertebrates. In: Berg, Jr., C.J. (Ed.), Culture of Marine Invertebrates. Hutchinson Ross Publishing Co., Stroudsberg, PA, pp. 108–132.

Holland, P.T., McNabb, P., Rhodes, L.L., Selwood, A.I., Neil, T., 2003. Amnesic shellfish poisoning toxins in New Zealand shellfish: detection of an unusual domoic acid isomer using a newly validated LC–MS/MS method. In: Villalba, A., Romalde Beiras, B.R.J. (Eds.), Molluscan Shellfish Safety. Xanta de Galicia & IOC of UNESCO, Santiago de Compostela, pp. 29–42.

Holland, P.T., Selwood, A.I., Mountfort, D.O., Wilkins, A.L., McNabb, P., Rhodes, L.L., Doucette, G.J., Mikulski, C.M., King, K.L., 2005. Isodomoic acid C, an unusual amnesic shellfish poisoning toxin from *Pseudo-nitzschia australis*. Chem. Res. Toxicol. 18, 814–816.

Kotaki, Y., 2008. Ecobiology of amnesic shellfish toxin producing diatoms. In: Botana, L.M. (Ed.), Seafood and Freshwater Toxins – Pharmacology, Physiology, and Detection. second ed. CRC Press, Taylor & Francis Group, New York, pp. 383–396.

Kotaki, Y., Lundholm, N., Katayama, T., Furio, E.F., Romero, M.L., Relox, J.R., Yasumoto, T., Naoki, H., Hirose, M.Y., Thann, T.D., Thuoc, C.V., Huyen, N.T.M., Thu, P.T., Takata, Y., Kodama, M., Fukuyo, Y., 2008. ASP toxins of pennate diatoms and bacterial effects on the variation in toxin composition. In: Moestrup, Ø., et al. (Eds.), Harmful Algae, The Proceeding of 12th International Conference on Harmful Algae. Intergovermental Oceanographic Commission, UNESCO, Copenhagen, Denmark, pp. 300–302.

Kotaki, Y., Furio, E.F., Satake, M., Lundholm, N., Katayama, T., Koike, K., Fulgueras, V.P., Bajarias, F.A., Takata, Y., Kobayashi, K., Sato, S., Fukuyo, Y., Kodama, M., 2005. Production of isodomoic acids A and B as major toxin components of a pennate diatom *Nitzschia navis-varingica*. Toxicon 46, 946–953.

Kotaki, Y., Koike, K., Yoshida, M., Thuoc, C.V., Huyen, N.T.M., Hoi, N.C., Fukuyo, Y., Kodama, M., 2000. Domoic acid production in *Nitzschia* sp. (Bacillariophyceae) isolated from a shrimp-culture pond in Do Son, Vietnam. J. Phycol. 36, 1057–1060.

Kotaki, Y., Lundholm, N., Onodera, H., Kobayashi, K., Bajarias, F.A., Furio, E.F., Iwataki, M., Fukuyo, Y., Kodama, M., 2004. Wide distribution of *Nitzschia navis-varingica*, a new domoic acid-producing benthic diatom found in Vietnam. Fish. Sci. 70, 28–32.

Lundholm, N., Moestrup, Ø., 2000. Morphology of the marine diatom *Nitzschia navis-varingica*, sp. nov, (Bacillariophyceae), another producer of the neurotoxin domoic acid. J. Phycol. 36, 1162–1174.

Lundholm, N., Skov, J., Pocklington, R., Moestrup, Ø., 1994. Domoic acid, the toxic amino acid responsible for amnesic shellfish poisoning, now in *Pseudonitzschia seriata* (Bacillariophyceae) in Europe. Phycologia 33, 475–478.

Maeda, M., Kodama, T., Tanaka, T., Yoshizumi, H., Takemoto, T., Nomoto, K., Fujita, T., 1986. Structures of isodomoic acids A B, and C, novel insecticidal amino acids from the red alga *Chondria armata*. Chem. Pharm. Bull. 34, 4892–4895.

Martin, J.L., Haya, K., Burridge, L.E., Wildish, D.J., 1990. *Nitzschia pseudodelicatissima* – a source of domoic acid in the Bay of Fundy, eastern Canada. Mar. Ecol. Prog. Ser. 67, 177–182.

Munday, R., Holland, P.T., McNabb, P., Selwood, A.I., Rhodes, L.L., 2008. Comparative toxicity to mice of domoic acid and isodomoic acids A, B and C. Toxicon 52, 954–956.

Orsini, L., Sarno, D., Procaccini, G., Poletti, R., Dahlmann, J., Montresor, M., 2002. Toxic *Pseudo-nitzschia multistriata* (Bacillariophyceae) from the Gulf of Naples: morphology, toxin analysis and phylogenic relationship with other *Pseudo-nitzschia* species. Eur. J. Phycol. 37, 247–257.

Pocklington, R., Milley, J.E., Bates, S.S., Bird, C.J., deFreitas, A.S.W., Quilliam, M.A., 1990. Trace determination of domoic acid in seawater and phytoplankton by high-performance liquid chromatography of the fluorenylmethoxycarbonyl (FMOC) derivative. Int. J. Environ. Anal. Chem. 38, 351–368.

Quilliam, M.A., 2003. Chemical methods for domoic acid, the amnesic shellfish poisoning (ASP) toxin. In: Hallegraeff, G.M., Anderson, D.M, Cembella, A.D. (Eds.), Manual on Harmful Marine Microalgae. UNESCO, Paris, pp. 247–265.

Rhodes, L., White, D., Syhre, M., Atkinson, M., 1996. *Pseudo-nitzschia* species isolated from New Zealand coastal waters: domoic acid production in vitro and links with shellfish toxicity. In: Yasumoto, T., Oshima, Y., Fukuyo, Y. (Eds.), Harmful and Toxic Algal Blooms. Intergovermental Oceanographic Commission of UNESCO, Paris, pp. 155–158.

Rhodes, L.L., 1998. Identification of potentially toxic *Pseudo-nitzschia* (Bacillariophyceae) in New Zealand coastal waters, using lectins. New Zeal. J. Mar. Freshwater Res. 32, 537–544.

Rhodes, L.L., Holland, P.T., Adamson, J.E., McNabb, P., Selwood, A.I., 2003. Production of a new isomer of domoic acid by New Zealand isolates of the diatom *Pseudo-nitzschia ausutralis*. In: Villalba, A.,Romalde, B.R.J.,Beiras, R. (Eds.),Molluscan Shellfish Safety. Xanta de Galicia & IOC of UNESCO, Santiago de Compostela, pp. 43–48.

Romero, M.L.J., Lirdwitayaprasit, T., Kotaki, Y., Lundholm, N., Relox, J.R., Furio, E.F., Terada, R., Yokoyama, T., Kodama, M., Fukuyo, Y., 2008. Isolation of ASP toxin-producing Nitzschia from Thailand. Mar. Res. Indones. 33, 225–228.

Takata, Y., Sato, S., Ha, D.V., Montojo, U.M., Lirdwitayaprasit, T., Kamolsiripichaiporn, S., Kotaki, Y., Fukuyo, Y., Kodama, M., 2009. Occurrence of domoic acid in tropical bivalves. Fish. Sci. 75, 473–480.

Takemoto, T., Daigo, K., 1958. Constituents of *Chondria armata*. Chem. Pharm. Bull. 6, 578–580.

Wright, J.L.C., Boyd, R.K., de Freitas, A.S.W., Falk, M., Foxall, R.A., Jamieson, W.D., Laycock, M.V., McCulloch, A.W., McInnes, A.G., Odense, P., Pathak, V.P., Quilliam, M.A., Ragan, M.A., Sim, P.G., Thibault, P., Walter, J.A., Gilgan, M., Richard, D.J.A., Dewar, D., 1989. Identification of domoic acid, a neuroexcitatory amino acid, in toxic mussels from eastern Prince Edward Island. Can. J. Chem. 67, 481–490.

Wright, J.L.C., Falk, M., McInnes, A.G., Walter, J.A., 1990. Identification of isodomoic acid D and two new geometrical isomers of domoic acid in toxic mussels. Can. J. Chem. 68, 22–25.

Zaman, L., Arakawa, O., Shimosu, A., Onoue, Y., Nishio, S., Shida, Y., Noguchi, T., 1997. Two new isomers of domoic acid from a red alga, *Chondria armata*. Toxicon 35, 205–212.

連載

社会と健康を科学するパブリックヘルス(4)
「コンピューターシミュレーションによる環境中化学物質のヒト曝露評価法」

京都大学大学院医学研究科環境衛生学分野　新添多聞　原田浩二　小泉昭夫

1. はじめに

現代社会において，おびただしい数の化学物質が活用され，常に新種の物質が生み出されている。特に近年の開発速度には目を見張るものがあるが，それは同時に環境中に排出される化学物質が増え続けているということでもある。現在，工業目的で使用されている化学物質はおよそ70000種あるとされており，ヒトの健康への影響が懸念されているものも少なくないが，その環境中での動態が明らかになっているものはわずかでしかない。

職業曝露を受けていない一般的なヒト集団の，環境中化学物質への曝露状況の実態を把握するには，実際のヒト集団から生体試料を採取することが最も有効であろう。京都大学大学院医学研究科では，ヒトの血液と陰膳法による食事試料を中心とする生体試料の収集を行ってきた。調査は1970年代に開始され，対象は日本国内のみならず，韓国，中国，ベトナムなど広く東アジアに及ぶ[1]。現在まで継続的に収集されてきた試料は京都大学生体試料バンクとして冷凍保存され，貴重なデータを提供している。しかしながら，このような調査で得られる情報は，調査が行われた地域，時代における情報でしかない。言うなれば，時間，空間について限定的かつ離散的な情報である。曝露状況を包括的に理解するにはこれらの範囲を広げるとともに，密度を向上させるべきであるが，財政的および人的資源が限られている中で，それは非常に困難であり，現実的でないとも言える。ここでは，コンピューターシミュレーションを活用してヒト曝露評価を行う手法である，Environmental ecological modeling（EEM）について紹介する。

2. EEMの概念と手法

EEMは3つのパートから構成される（図1）。大気輸送モデル，体内動態モデル，生体試料である。環境中化学物質に対するヒトの曝露経路には大きく分けて2つある。呼吸による吸入摂取と，食事による消化管摂取である。吸入摂取は化学物質の大気中濃度に依存するが，これは大気の流れによって輸送されるため排出源の影響が広範囲に及び，国境を越えることも少なくない。一方，消化管摂取は化学物質の食料，飲料水中の含有量に依存するが，これはそれぞれの国における供給体制を反映するものと考えられる。

そこで，吸入摂取量は大気輸送モデルにより計算した大気中濃度に基づいて算出する。その際，大気への排出の強度，分布，時間による推移は，その物質の排出に関する知見と経済統計などから推定し，大気モデルに入力する。従って，吸入摂取量は位置と時間の関数として与えられる。消化管摂取量は生体試料バンクの陰膳食事試料における含有量の実測値に基づいて算出し，国ごとに時間の関数として与える。算出した吸入および消化管摂取量をヒトの体内動態モデルに入力し，血（清）中濃度を計算する。

この計算値を，生体試料バンクの血液試料における濃度と比較して検証を行う。計算値と実測値がうまく一致していれば，大気モデル，体内動態モデルともに正しく機能しているということになる。そして検証されたモデルの結果を解析すれば各地域の任意の時間におけるヒト曝露状況を評価することができる。

図1　EEMの概念図。

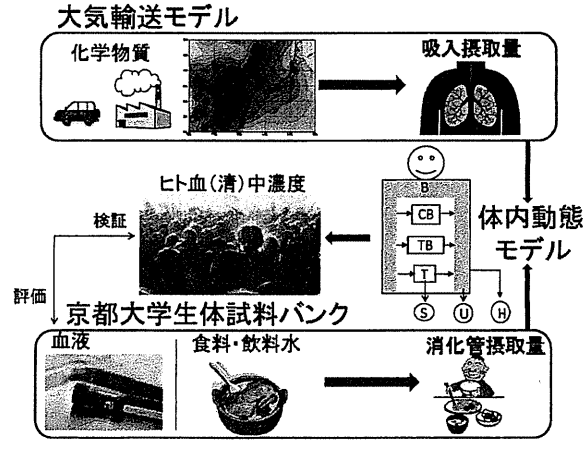

3. EEMの適用例-血中鉛のシミュレーションと曝露評価

EEMの適用例として，血中鉛のシミュレーションを紹介する。鉛は古くから工業目的で広く活用され，有毒な重金属としては環境中に最も多量に存在する。大気中では微小粒子中に含まれ，広範囲に輸送される。大気への排出は有鉛ガソリンの使用によるものが最も多く，次いで非鉄金属の精錬工程からのものが多い。さらに近年は石炭などの化石燃料燃焼の影響も指摘されている。多くの先進国では有鉛ガソリンの禁止など環境中鉛の排出削減努力により既に大きな成果が得られている。一方，東アジアでは削減がいまだ不十分な国が少なくなく，そういった中で急速な経済成長が進行している。我が国における大気を通じた越境汚染も懸念されており，ヒト曝露の実態把握が急がれる。そこで筆者らはEEMを用いて，日本，韓国，中国，ベトナムにおける成人女性の過去の血中鉛濃度の再現を行い，環境中鉛に対する曝露評価を行った[2]。対象期間は1979年から2009年である。

3-1. シミュレーション

大気モデルには水平解像度1.25度の全球輸送モデルを用いた。既存のデータや経済統計などを基に4カ国からの鉛排出量を推定して大気モデルに入力し，大気中濃度分布を計算して過去30年間の観測データと比較したところ，概ね良い一致が見られた[2,3]。各地の鉛の吸入摂取量はこのモデルによる地表面大気中濃度から算出した。消化管摂取量は，生体試料バンクの食事試料における鉛含有量データに対して，各国ごとに指数回帰を適用し，時間の関数として算出した。

算出した鉛摂取量を，4つの体内区画から成る動態モデル[4]に入力して血中鉛濃度を計算した。4カ国の成人女性の血中鉛濃度の計算値を実測値と比較した（図2）。実測データにおける血中濃度の幾何平均（GM）値は，日本では1980年頃に32.8 $\mu g\ L^{-1}$であったのが1990年代には24.0 $\mu g\ L^{-1}$に減少し，その後2000年代には15.7 $\mu g\ L^{-1}$まで減少している。韓国でのGM値は1994年の44.3 $\mu g\ L^{-1}$から2000年代には17.7 $\mu g\ L^{-1}$まで減少した。中国のGM値は1980年代は60.5 $\mu g\ L^{-1}$，1990年代は53.6 $\mu g\ L^{-1}$，2000年代は53.9 $\mu g\ L^{-1}$である。ベトナムでは2009年のGM値は28.0 $\mu g\ L^{-1}$であり，これは1980年頃の日本，あるいは2000年代初頭の韓国の水準に近い。EEMは過去の実測値のほとんどすべてを2倍の誤差の範囲で再現できていることが分かる。

3-2. 曝露評価

図3は東京，ソウル，北京，ハノイにおける成人女性の血中鉛濃度の計算値（$\mu g\ L^{-1}$）の推移である。計算値に見られる振動は地表面大気中鉛濃度の季節変化によるもので，冬季に極大となることが多い。呼吸による吸入摂取量を含まない場合（no-air run）の結果も図中に示す。control runとno-air runの差が，血中鉛全体に対する大気由来成分の寄与を表すことになる。

東京での計算値は1980年の44 $\mu g\ L^{-1}$から2009年の18 $\mu g\ L^{-1}$まで58％減少している。ソウルでは1990年代初頭は50 $mg\ L^{-1}$を超えていたのが，2009

図2　成人女性の血中鉛濃度の計算値と実測値との比較（$\mu g\ L^{-1}$）。中央の実線は計算値と実測値が一致すること，2本の破線は誤差が2倍であることを表す。（+）日本1980年頃，（●）日本1990年代，（×）日本2000年以降，（□）韓国2000年以前，（@）韓国2000年以降，（△）中国1980年代，（＊）中国1990年代，（○）中国2005年以降，（V）ベトナム2005年以降。

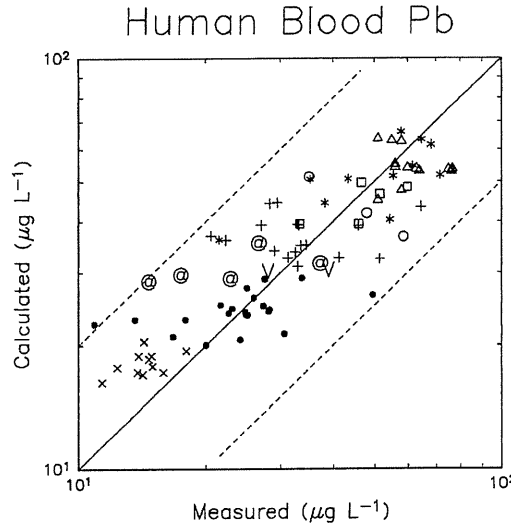

図3　モデルによる，東京，ソウル，北京，ハノイにおける成人女性の血中鉛濃度の1979年から2009年までの推移。破線は呼吸器からの曝露を含まない場合（no-air）の計算値。

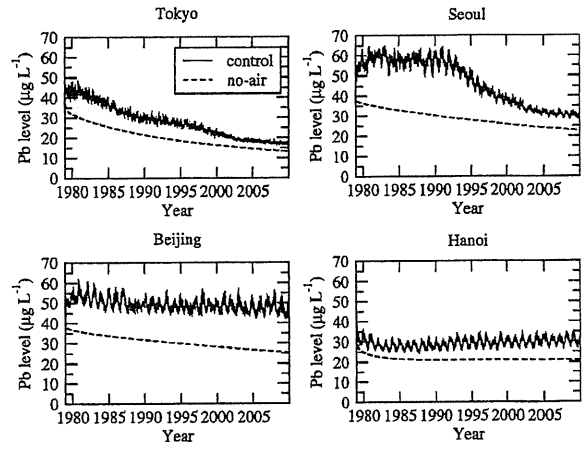

年には29 $\mu g\,L^{-1}$ となり45%の減少である。東京での大気由来成分の寄与は小さく，1983年の30%から2003年の19%の範囲である。ソウルでは1990年に48%であったのが2005年の24%まで減少している。北京における血中鉛濃度の計算値はおよそ50 $\mu g\,L^{-1}$ で，現在の東京の計算値よりずっと大きい。計算値の減少の度合いが東京やソウルより緩やかであることは，実測値の経年変化が中国では日本や韓国ほどはっきりしない（図2）ことと整合性がとれている。北京では大気由来成分の寄与は1980年の32%から2009年の43%へと増加している。ハノイでは鉛の大気への排出量と食料，飲料水中含有量が一定であると仮定したときの血中濃度の計算値はおよそ30 $\mu g\,L^{-1}$ で，大気由来成分の寄与は30%である。血中濃度も大気由来成分の寄与も現在のソウルでの計算値と同程度である。しかしながら，トレンドに関しては，継続的な測定データがなければ評価することはできない。

東京，ソウルにおける成人女性の血中鉛濃度のモデル値に減少トレンドが見られたのは日本，韓国における環境中鉛の削減を反映するものである。有鉛ガソリンが禁止された時期を含む10年間の血中鉛濃度の減少の大きさは，東京で1980年から1990年にかけて30.6%，ソウルで1990年から2000年にかけて37.8%である。これは先進国で実際に見られた減少率に近い値である。例えば米国では1991年から1994年の調査と1999年から2002年の調査の結果では30.2%減少しており[5]，ドイツでは1990年から1992年の調査と1998年の調査の結果では30.5%減少している[6]。

モデルによる北京の血中鉛濃度は他の都市の現在の血中濃度よりずっと高い。また1999年から2009年にかけて，モデル値はわずか4.1%減少したに過ぎない。また，大気由来成分の寄与もはっきりと増加している。中国の有鉛ガソリンは2001年に禁止されているが，北京の大気中鉛濃度は近年漸増していることが観測されており，石炭消費量の増加によるものと考えられている[7]。今後，中国の急激な経済成長により，中国だけでなく周辺国でも大気中濃度が大きく増加する可能性が否定できない。従って，東アジア全体で環境中鉛を継続的にモニターしていく必要がある。

4. EEMの展望

EEMは関西地方におけるパーフルオロオクタン酸（PFOA）の血清中濃度のシミュレーションに初めて使用された[8]。ある化学工場からのPFOAの排出量，大気による輸送量および周辺住民の曝露量を評価した。これにより周辺住民の血清中に見られた高いPFOA濃度の原因が明らかになった。鉛に関しては，ハノイ市の児童におけるリスク評価にも応用している[2]。血液と食における汚染レベルについての情報があれば，EEMは他の物質や地域にも適用できる。さらに，過去のトレンドや現在のリスクを評価するだけでなく，未知の汚染源の推定や，曝露シナリオを想定しての将来のトレンドやリスクの予測を行うこともできる。また実行に際して，財政的負担が小さいことも指摘しておくべきであろう。生体試料により得られる情報は極めて重要ではあるが，時間，空間について限定的，離散的であると先に述べた。以上見てきたように，EEMはコンピューターを活用することにより，限定的，離散的情報を包括的，連続的情報に拡張して活用する手法であるとも言え，環境評価や政策決定にも大いに貢献できるものと確信している。

文　献

1) Koizumi A., Harada K., Inoue K., Hitomi T., Yang H.-R., Moon C.-S., Wang P., Hung N. N., Watanabe T., Shimbo S., Ikeda M., Past, present, and future of environmental specimen banks. *Environ. Health Prev. Med.* 2009, *14*, 307–318.

2) Niisoe T., Harada K. H., Hitomi T., Watanabe T., Hung N. N., Ishikawa H., Wang Z., Koizumi A., Environmental ecological modeling of human blood lead levels in East Asia, *Environ. Sci. Technol.* 2011, in press.

3) Niisoe T., Nakamura E., Harada K., Ishikawa H., Hitomi, T., Watanabe T., Wang Z., Koizumi A., A global transport model of lead in the atmosphere. *Atmos. Environ.* 2010, *44*, 1806–1814.

4) Marcus A. H., Multicompartment kinetics models for lead, II. Linear kinetics and variable absorption in humans without excessive lead exposure. *Environ. Res.* 1985, *36*, 459–471.

5) Centers for Disease Control and Prevention, Blood lead levels—United States, 1999–2002. *MMWR. Morb. Mortal. Wkly. Rep.* 2005, *54*(20), 513–516.

6) Trends: German Environmental Survey 1998 (GerES III), Health and Environmental Hygiene. www.umweltbundesamt.de/gesundheit-e/survey/vergleich/zvergleich.htm.（2011年2月18日アクセス可能）

7) Okuda T., Katsuno M., Naoi D., Nakao S., Tanaka S., He K., Ma Y., Lei Y., Jia Y., Trends in hazardous trace metal concentrations in aerosols collected in Beijing, China from 2001 to 2006. *Chemosphere* 2008, *72*, 917–924.

8) Niisoe T., Harada K. H., Ishikawa H., Koizumi A., Long-term simulation of human exposure to atmospheric perfluorooctanoic acid (PFOA) and perfluorooctanoate (PFO) in the Osaka urban area, Japan. *Environ. Sci. Technol.* 2010, *44*, 7852–7857.